POLITECNICO DI MILANO

MEMS modelling and design group

Centre for Computational Structural and Materials Mechanics

Overall mechanical properties of polysilicon films: homogenization vs Monte Carlo simulations

Stefano Mariani

F. Confalonieri, A. Corigliano, M. Dossi, A. Ghisi

Politecnico di Milano

Dipartimento di Ingegneria Civile e Ambientale

ISFH

Workshop

Impact of mechanical and thermal loads on the long term stability of PV modules

ENGINEERING MOTIVATION:
failure of POLYSILICON inertial MEMS sensors exposed to accidental drops or shocks

Due to accidental drops/shocks,
the most stressed details of inertial MEMS sensors (suspension springs) can break because of the propagation of inter- and/or trans-granular cracks

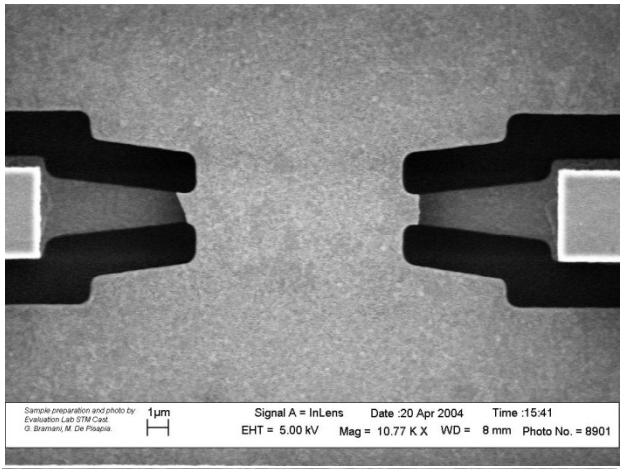

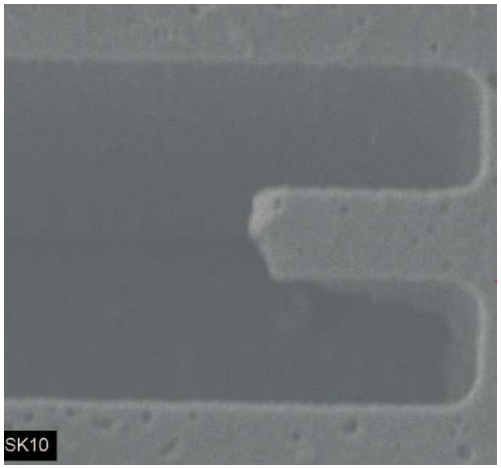

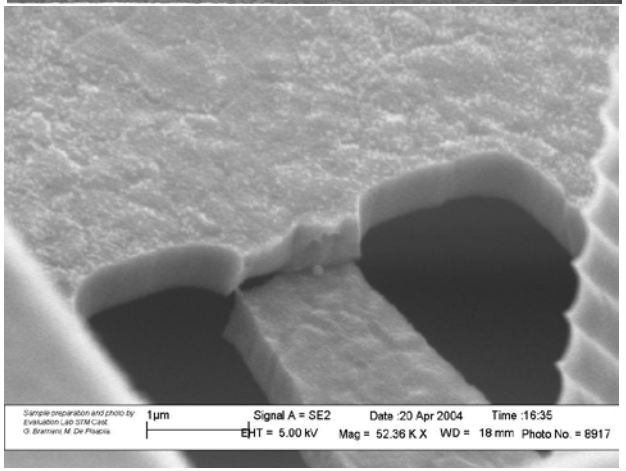

Microsystems fabrication

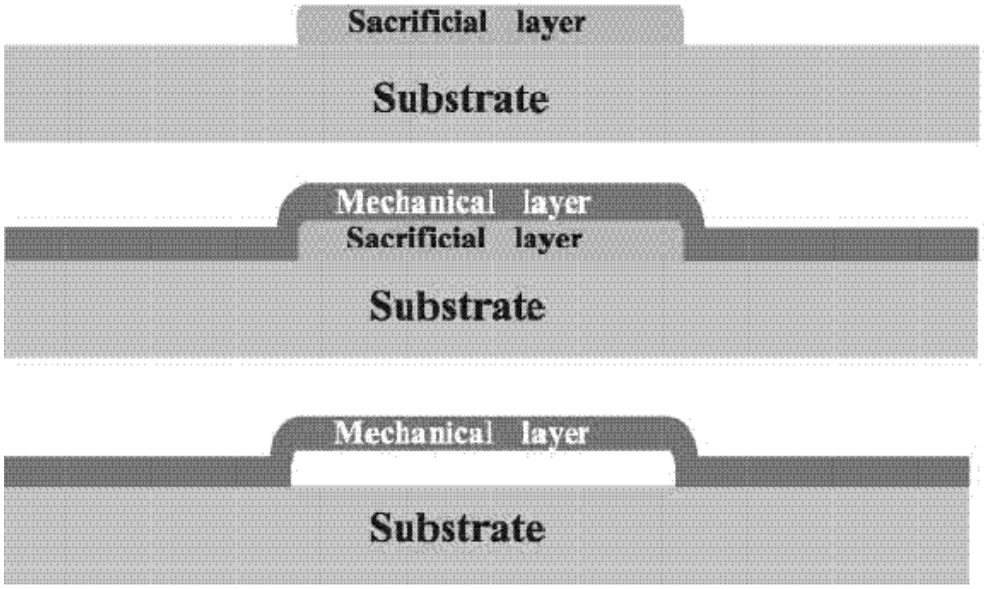

deposition of the oxide sacrificial layer

deposition of the silicon structural layer

oxide Removal

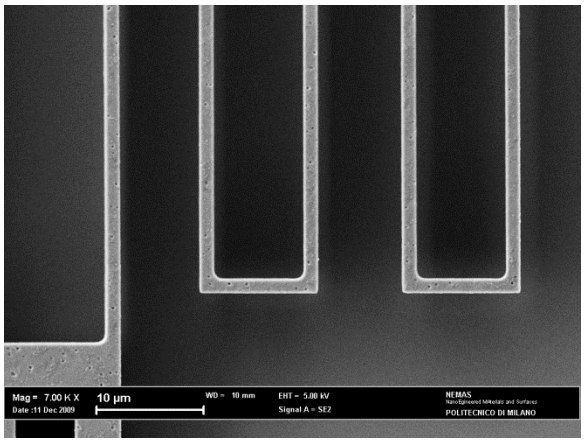

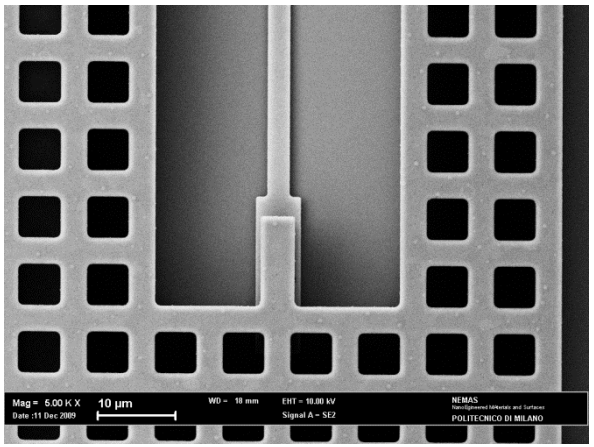

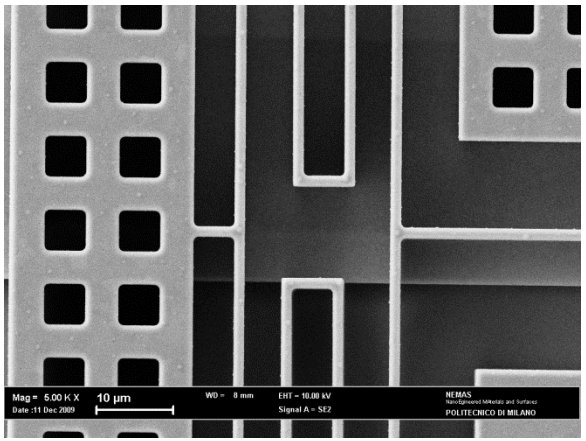

Length-scales in packaged MEMS

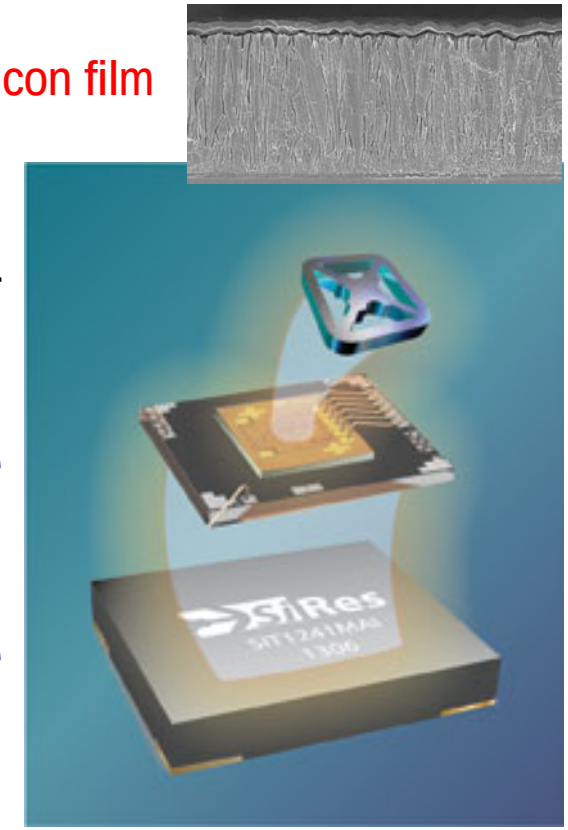

Multi-scale analysis of MEMS subject to impacts:

- decoupling between macro-scale and meso-scale allowed by small inertia of the sensor
- decoupling between meso-scale and micro-scale? (not allowed if nonlinear effects to be simulated)

	mass (Kg)
Package	$5 \cdot 10^{-4}$
Die	$2.3 \cdot 10^{-6}$
Sensor	$3 \cdot 10^{-9}$

Multi-scale analysis of shock-induced failure of polysilicon MEMS accelerometers

Two-scales

Industry-oriented approach for design and testing

macro

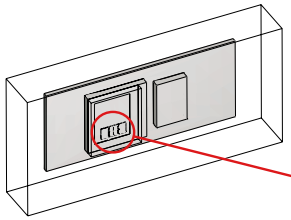

meso

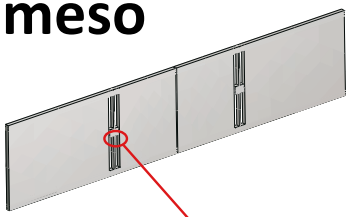

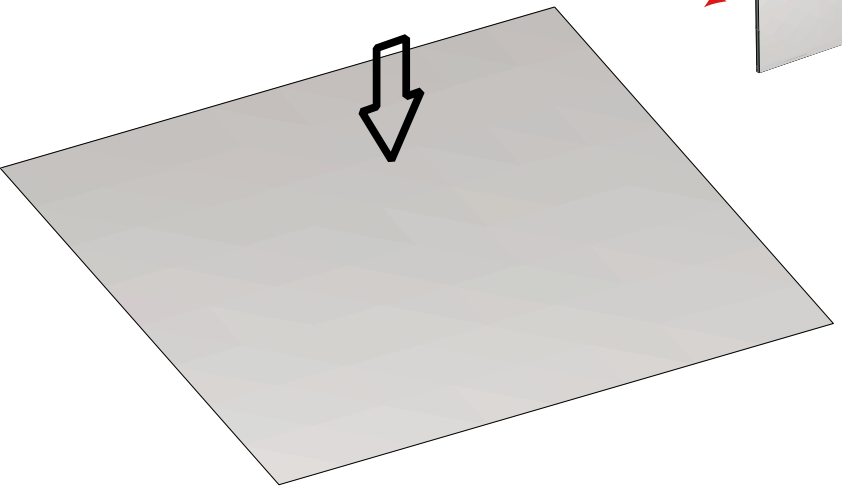

micro

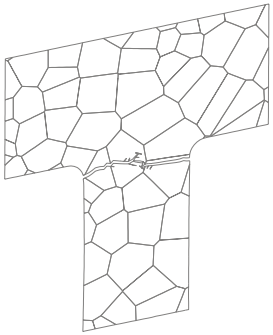

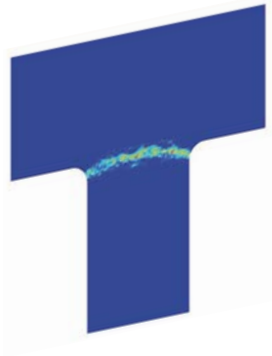

Simplified top-down approach

Three-scales

Understanding the underlying failure mechanisms

On-chip testing (crack and fatigue)

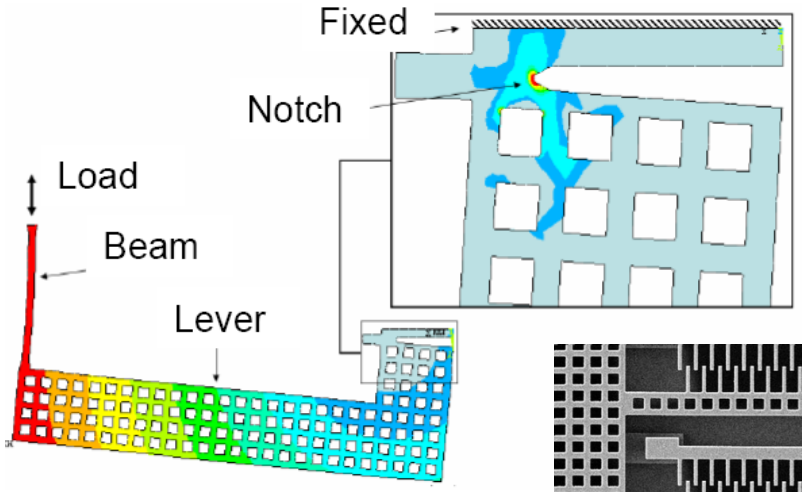

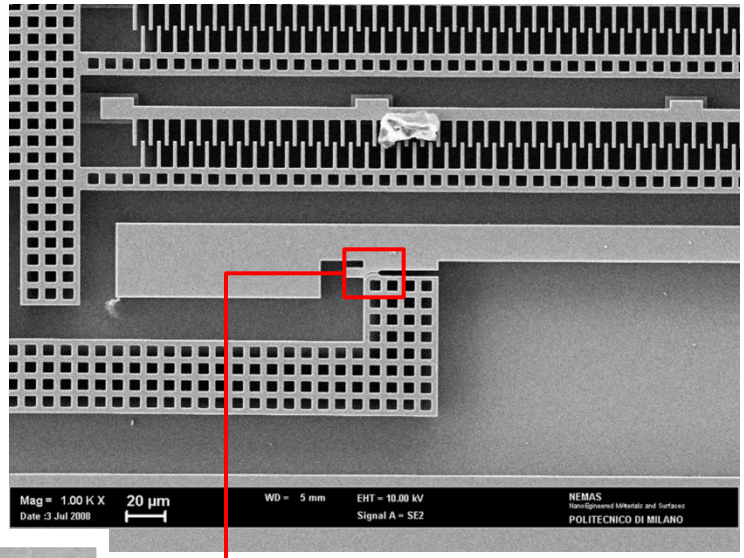

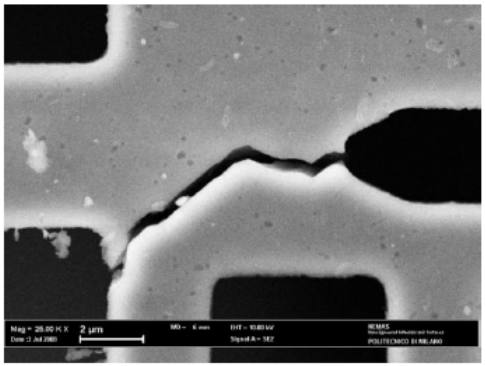

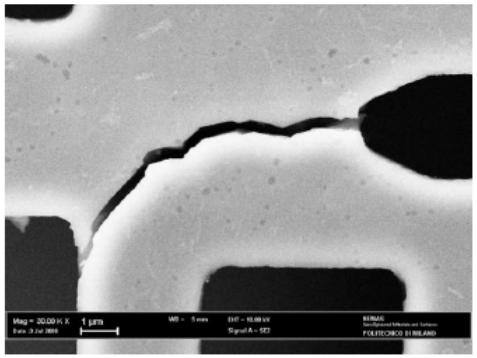

Multi-scale analysis (2S vs 3S)

MACRO-SCALE simulations:
effect of drop features (drop height, falling orientation) on acceleration/displacement histories at anchors.
Tool: commercial FE code, 3D models

MESO-SCALE simulations:
link between drop features (drop height, falling orientation) and sensor failure probability. In 3S analyses, localization of most stressed sensor regions and input definition for micro-scale analysis.
Tool: commercial FE code, 3D models + material **failure criterion**

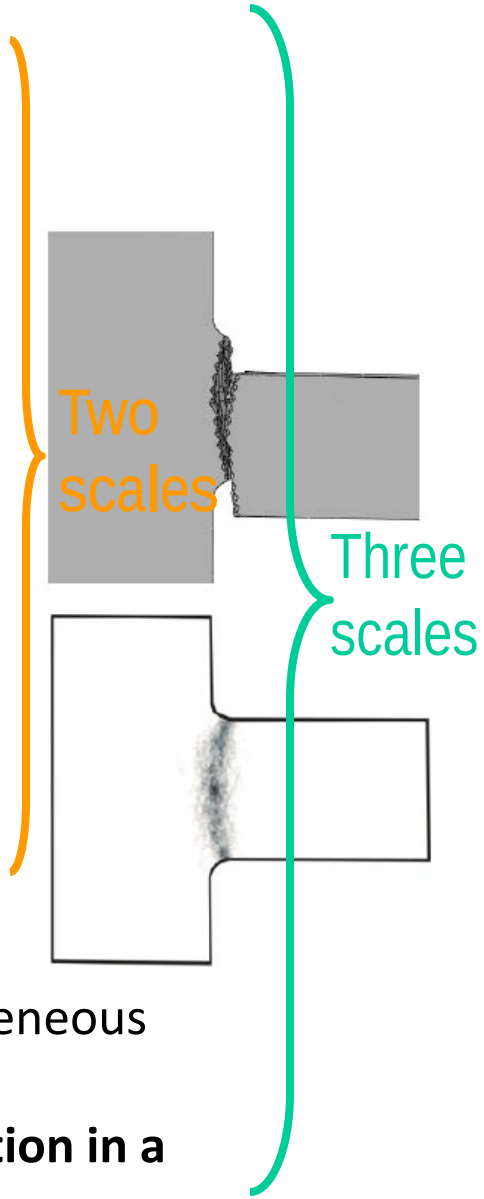

MICRO-SCALE simulations:
influence of the microstructure on failure mechanisms, heterogeneous (polycrystalline) material.
Tool: research code to **simulate fracture initiation and propagation in a polycrystal**, **Monte Carlo** simulations

References

1. S. Mariani, A. Ghisi, A. Corigliano, S. Zerbini. Multi-scale analysis of MEMS sensors subject to drop impacts. *Sensors*, **7**, pp. 1817-1833, 2007.
2. S. Mariani, A. Ghisi, F. Fachin, F. Cacchione, A. Corigliano, S. Zerbini. A three-scale FE approach to reliability analysis of MEMS sensors subject to impacts. *Meccanica*, **43**, pp. 469-483, 2008.
3. A. Ghisi, F. Fachin, S. Mariani, S. Zerbini. Multi-scale analysis of polysilicon MEMS sensors subject to accidental drops: Effect of packaging. *Microelectronics Reliability*, **49**, pp. 340-349, 2009.
4. S. Mariani, A. Ghisi, A. Corigliano, S. Zerbini. Modeling impact-induced failure of polysilicon MEMS: a multi-scale approach. *Sensors*, **9**, pp. 556-567, 2009.
5. S. Mariani, R. Martini, A. Ghisi, A. Corigliano, B. Simoni. Monte Carlo simulation of micro-cracking in polysilicon MEMS exposed to shocks. *International Journal of Fracture,* **167**, pp. 83-101, 2011.
6. A. Ghisi, S. Kalicinski, S. Mariani, I. De Wolf, A. Corigliano. Polysilicon MEMS accelerometers exposed to shocks: numerical-experimental investigation. *Journal of Micromechanics and Microengineering*, **19**, 035023, 2009.
7. S. Mariani, A. Ghisi, A. Corigliano, R. Martini, B. Simoni. Two-scale simulation of drop-induced failure of polysilicon MEMS sensors. *Sensors*, **11**, pp. 4972-4989, 2011.
8. A. Ghisi, S. Mariani, A. Corigliano, S. Zerbini. Physically-based reduced order modelling of a uni-axial polysilicon MEMS accelerometer. *Sensors*, **12**, pp. 13985-14003, 2012.
9. S. Mariani, R. Martini, A. Ghisi, A. Corigliano, M. Beghi. Overall elastic properties of polysilicon films: a statistical investigation of the effects of polycrystal morphology. *International Journal for Multiscale Computational Engineering,* **9**, pp. 327-346, 2011.
10. S. Mariani, R. Martini, A. Corigliano, M. Beghi. Overall elastic domain of thin polysilicon films**.** *Computational Materials Science*, **50**, pp. 2993-3004, 2011.
11. F. Confalonieri. A domain decomposition approach for the simulation of fracture phenomena in polycrystalline microsystems. *PhD Thesis*, 2013.
12. F. Confalonieri, G. Cocchetti, A. Ghisi, A. Corigliano. A domain decomposition method for the simulation of fracture in polysilicon MEMS. *Microelectronics Reliability*, in press.
13. A. Corigliano, M. Dossi, S. Mariani. Domain decomposition and model order reduction methods applied to the simulation of multiphysics problems in MEMS. *Computers and Structures*, **122**, pp. 113–127, 2013.

Overview of a studied device (uni-axial MEMS accelerometer)

- Package (macro-scale)

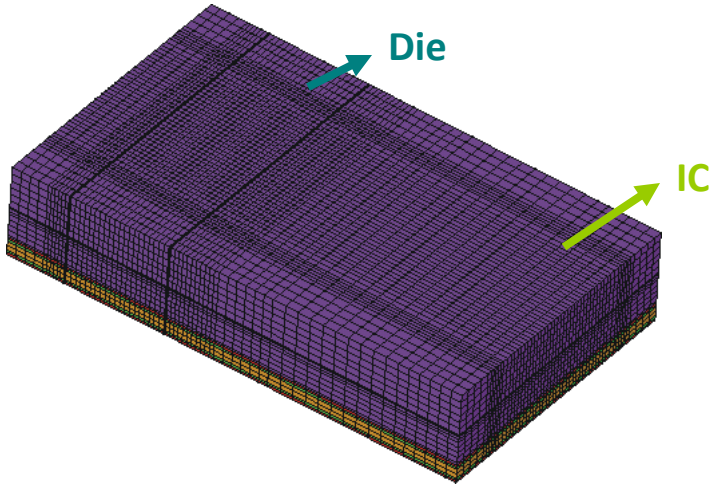

- Die (macro-scale)

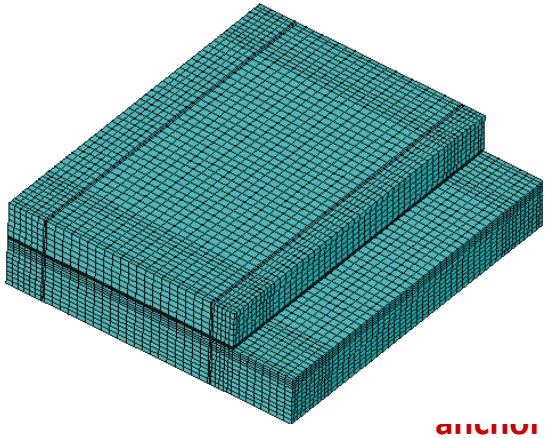

- Sensor (meso-scale)

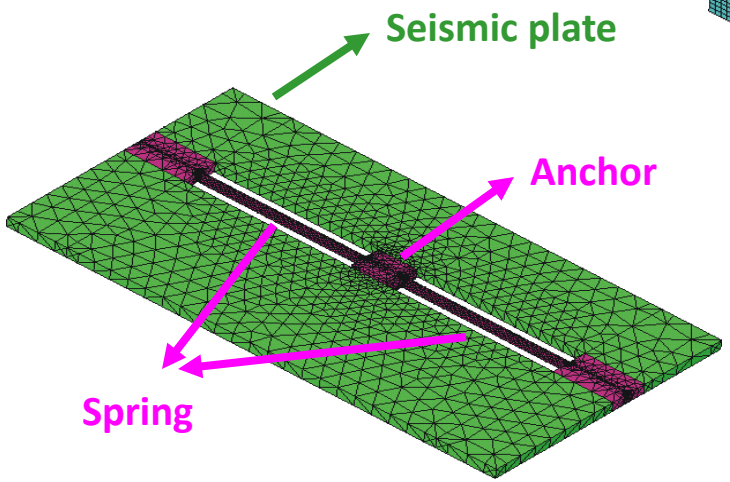

Two-scale vs three-scale analysis of drop-induced effects

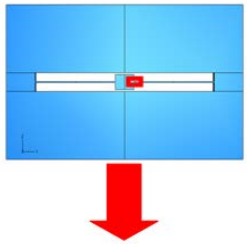

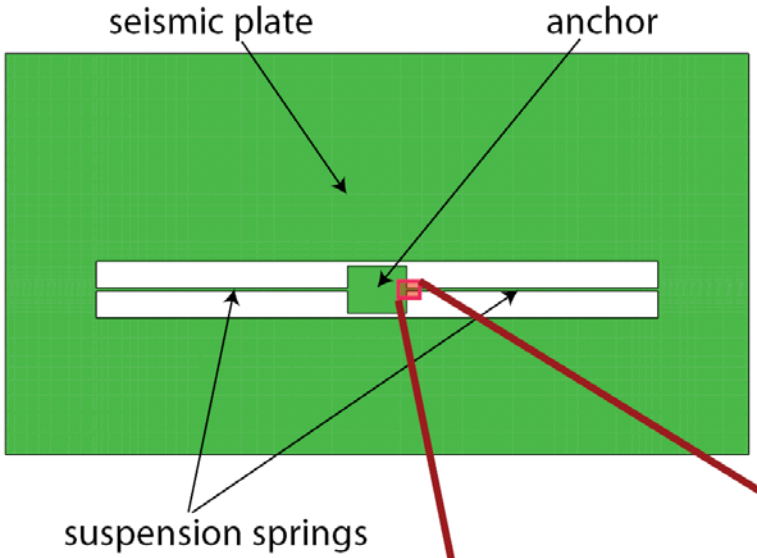

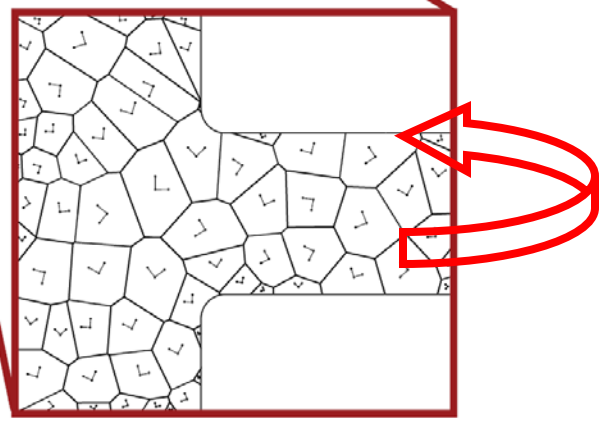

The falling direction leads to bending-dominated deformation of the suspension springs (two-dimensional analysis at micro-scale allowed)

Meso-scale analyses: results

Adopted space discretization ($d_e = 100$ nm)

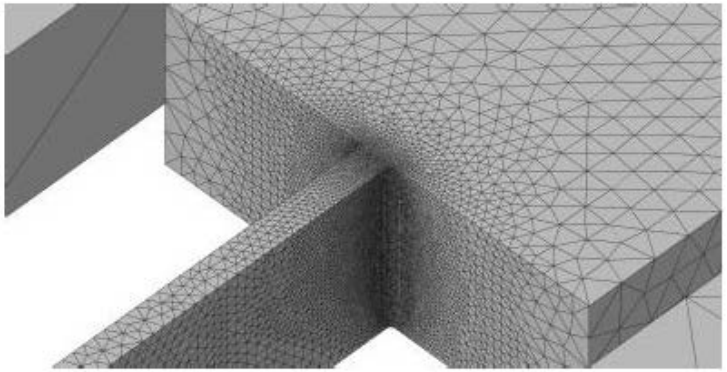

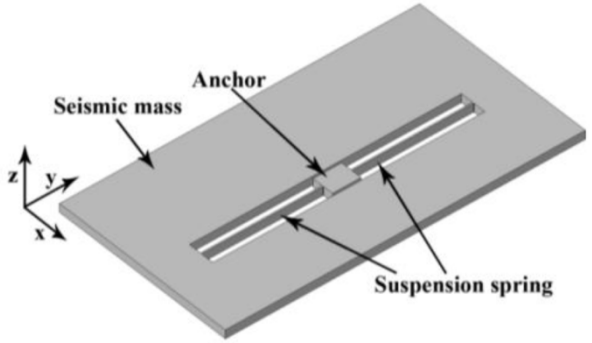

Local stress intensification close to the anchor point

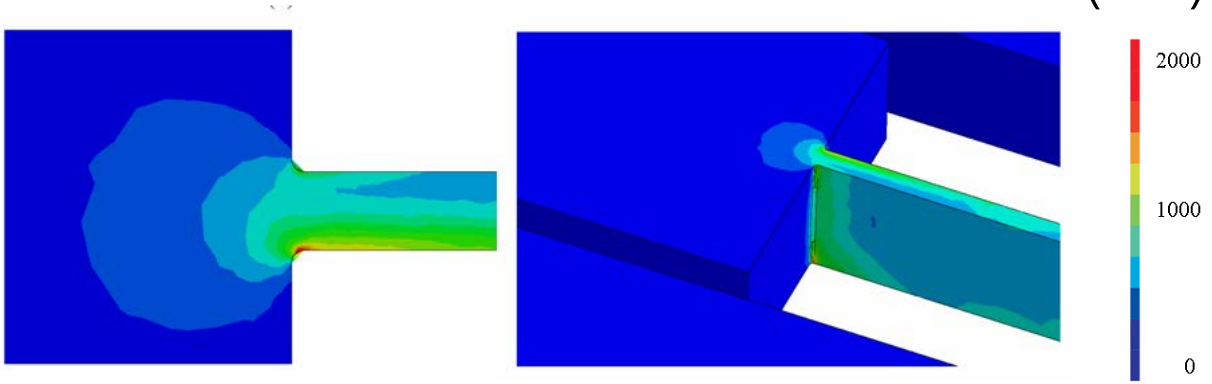

Forecasted failure mode (smeared-crack approach using Abaqus)

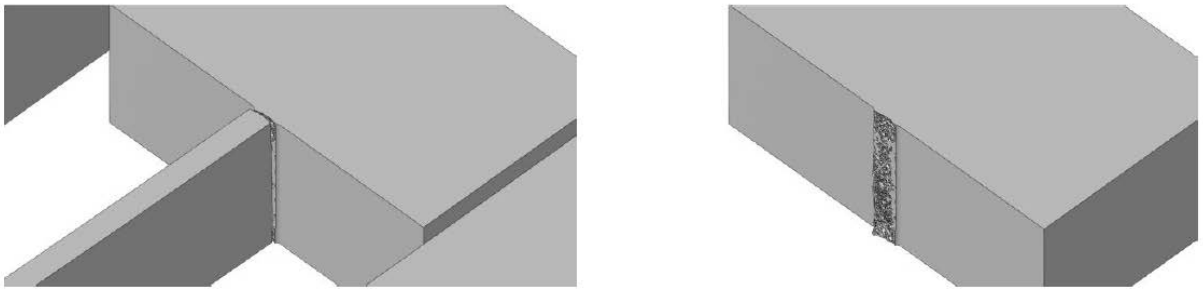

Micro-scale vs meso-scale results

tension-dominated loading

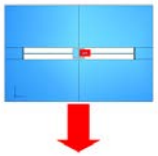

bending-dominated loading

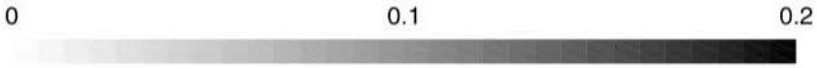

Micro-scale:
loci of max failure probability due to quasi-brittle cracking

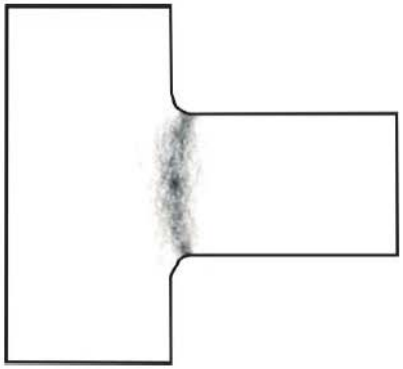

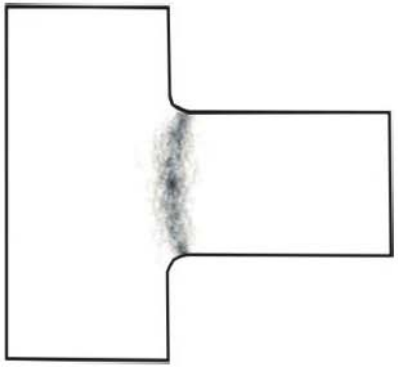

Meso-scale:
failure mode due to brittle cracking

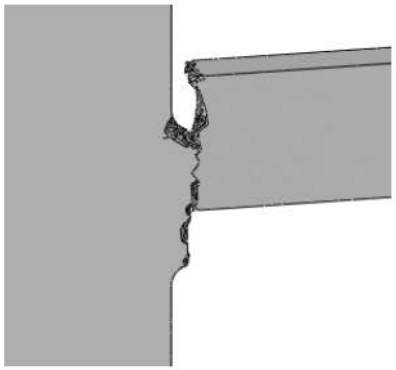

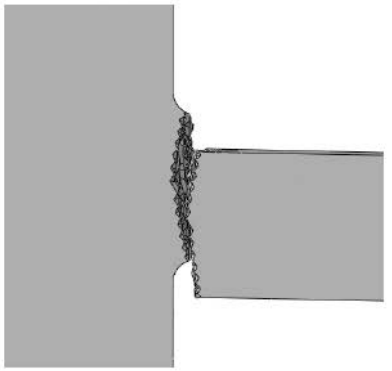

Topics to discuss:

1. Meso-scale elastic properties
2. Meso-scale elastic domain (strength)
3. Micro-scale quasi-brittle cracking

Meso-scale elastic properties

Micro-scale analysis: upscaling of elastic properties

Columnar polysilicon film
(lateral view)

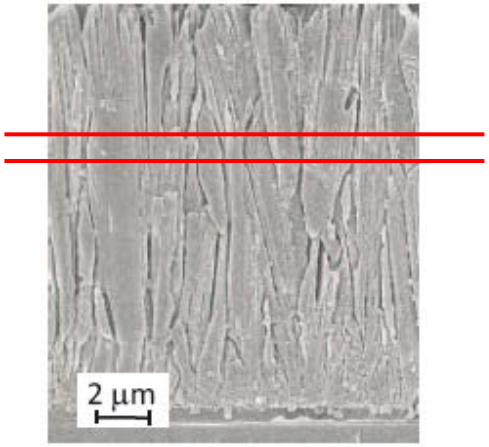

taking a slice of the film
(plane stress cond.)

regularized Voronoi tessellations

Through homogenization: in-plane macro strain and stress vectors

$$\boldsymbol{E} = \{E_{11} \;\; E_{22} \;\; E_{12}\}^{\mathrm{T}}$$
$$\boldsymbol{\Sigma} = \{\Sigma_{11} \;\; \Sigma_{22} \;\; \Sigma_{12}\}^{\mathrm{T}}$$

defined as volume averages, according to:

$$\boldsymbol{\Sigma} = \frac{1}{V}\int_V \boldsymbol{\sigma} dV$$

$$\boldsymbol{E} = \frac{1}{V}\int_V \boldsymbol{\varepsilon} dV$$

local elastic law

$$\boldsymbol{\sigma} = \boldsymbol{c}\boldsymbol{\varepsilon}$$

Micro-scale: polysilicon properties

Polysilicon assumed to feature:

- one axis of elastic symmetry aligned with epitaxial growth direction x_3
- random orientation of other two elastic symmetry directions in the x_1- x_2 plane

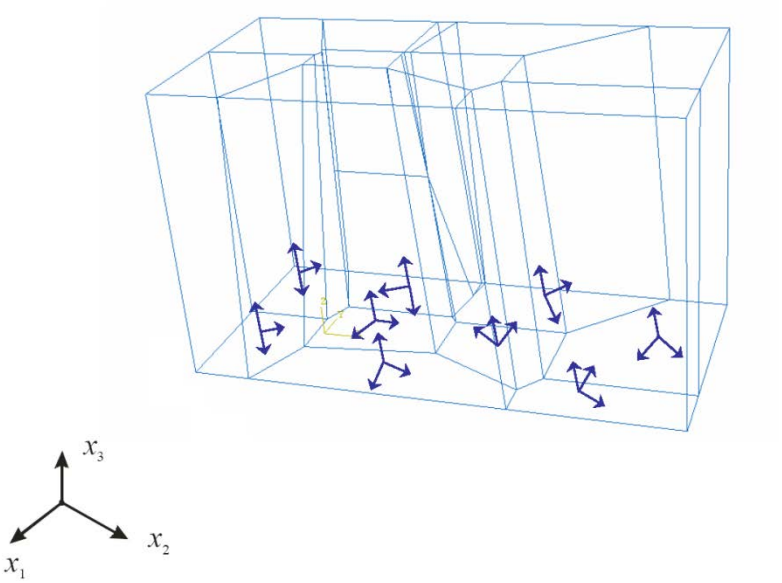

Matrix of elastic moduli for single-crystal Si (FCC symmetry)

$$\mathbf{c} = \begin{bmatrix} 165.7 & 63.9 & 63.9 & 0 & 0 & 0 \\ 63.9 & 165.7 & 63.9 & 0 & 0 & 0 \\ 63.9 & 63.9 & 165.7 & 0 & 0 & 0 \\ 0 & 0 & 0 & 79.6 & 0 & 0 \\ 0 & 0 & 0 & 0 & 79.6 & 0 \\ 0 & 0 & 0 & 0 & 0 & 79.6 \end{bmatrix} \; GPa$$

Reference value for nominal tensile strength (depending on the local loading mode)

$$\sigma_c = 2 \div 4 \text{ GPa}$$

Micro-scale analysis: upscaling of elastic properties

Elastic moduli in $\Sigma = CE$ are numerically bounded through:

- uniform strain boundary cond.

$$\boldsymbol{u} = \boldsymbol{X}\boldsymbol{E} \quad \text{on} \quad \partial V$$

- uniform stress boundary cond.

$$\boldsymbol{T} = \boldsymbol{N}\boldsymbol{\Sigma} \quad \text{on} \quad \partial V$$

$$\boldsymbol{X} = \begin{bmatrix} x_1 & 0 & \frac{x_2}{2} \\ 0 & x_2 & \frac{x_1}{2} \end{bmatrix}$$

$$\boldsymbol{N} = \begin{bmatrix} n_1 & 0 & n_2 \\ 0 & n_2 & n_1 \end{bmatrix}$$

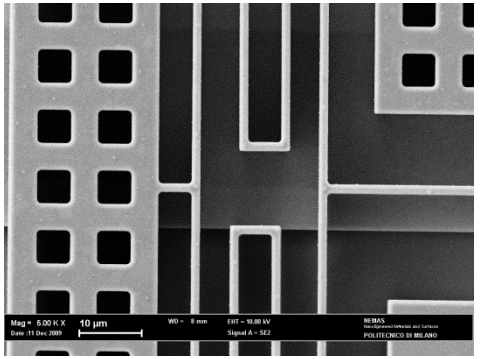

Voigt and **Reuss** bounds:
from Hill-Mandel macro-homogeneity condition $\boldsymbol{\Sigma}^{\mathrm{T}}\boldsymbol{E} = \frac{1}{V}\int_V \boldsymbol{\sigma}^{\mathrm{T}}\boldsymbol{\varepsilon}\,dV = \frac{1}{V}\int_V \boldsymbol{\sigma}_l^{\mathrm{T}}\boldsymbol{\varepsilon}_l\,dV$

Voigt assumption: $\boldsymbol{\varepsilon} = \boldsymbol{E}$ everywhere

$$\boldsymbol{E}^{\mathrm{T}}\boldsymbol{C}\boldsymbol{E} = \frac{1}{V}\int_V \boldsymbol{\varepsilon}_l^{\mathrm{T}}\boldsymbol{c}_l\boldsymbol{\varepsilon}_l\,dV = \frac{1}{V}\int_V \boldsymbol{\varepsilon}^{\mathrm{T}}\boldsymbol{t}_\varepsilon^{\mathrm{T}}\boldsymbol{c}_l\boldsymbol{t}_\varepsilon\boldsymbol{\varepsilon}\,dV = \boldsymbol{E}^{\mathrm{T}}\left[\frac{1}{V}\int_V \boldsymbol{t}_\varepsilon^{\mathrm{T}}\boldsymbol{c}_l\boldsymbol{t}_\varepsilon\,dV\right]\boldsymbol{E} = \boldsymbol{E}^{\mathrm{T}}\left[\frac{1}{V}\int_V \boldsymbol{c}\,dV\right]\boldsymbol{E}$$

$$\Rightarrow \quad \boldsymbol{C} = \frac{1}{V}\int_V \boldsymbol{t}_\varepsilon^{\mathrm{T}}\boldsymbol{c}_l\boldsymbol{t}_\varepsilon\,dV$$

Reuss assumption: $\boldsymbol{\sigma} = \boldsymbol{\Sigma}$ everywhere $\quad \Rightarrow \quad \boldsymbol{C}^{-1} = \frac{1}{V}\int_V \boldsymbol{t}_\sigma^{\mathrm{T}}\boldsymbol{c}_l^{-1}\boldsymbol{t}_\sigma\,dV$

Micro-scale analysis: upscaling of elastic properties

$L = 12\ \mu\text{m},$
$\bar{s}_g = 0.2\ \mu\text{m}$

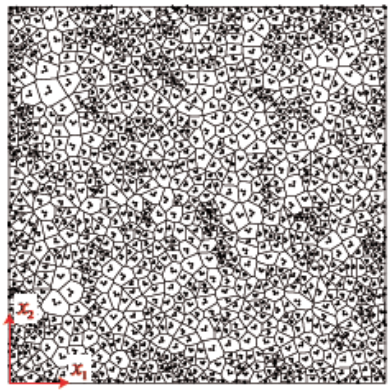

$\boldsymbol{u} = \boldsymbol{X}\boldsymbol{E}$ on ∂V

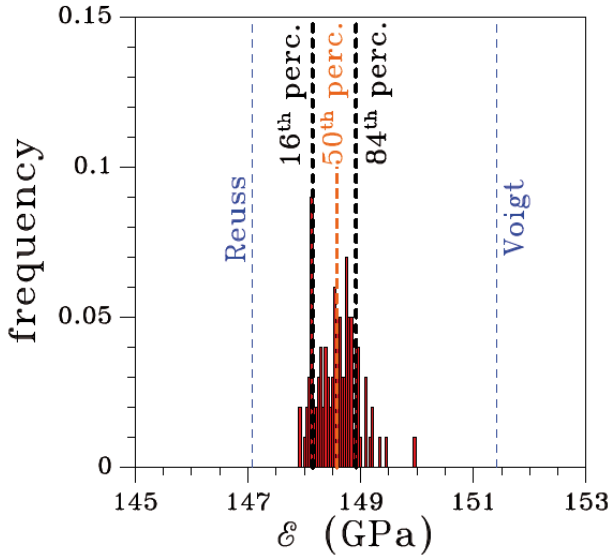

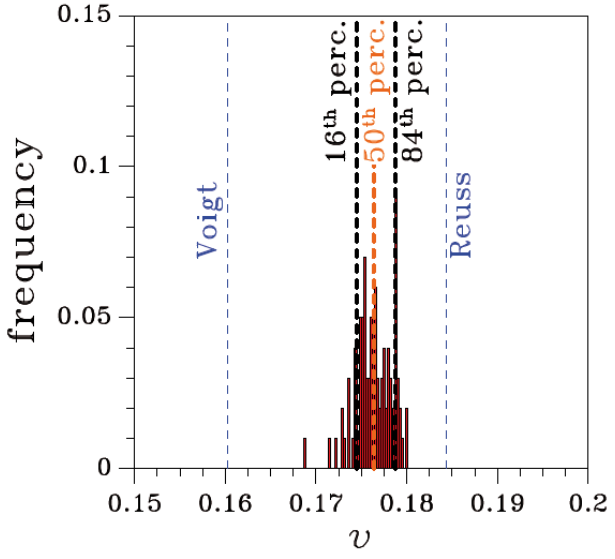

$\boldsymbol{T} = \boldsymbol{N}\boldsymbol{\Sigma}$ on ∂V

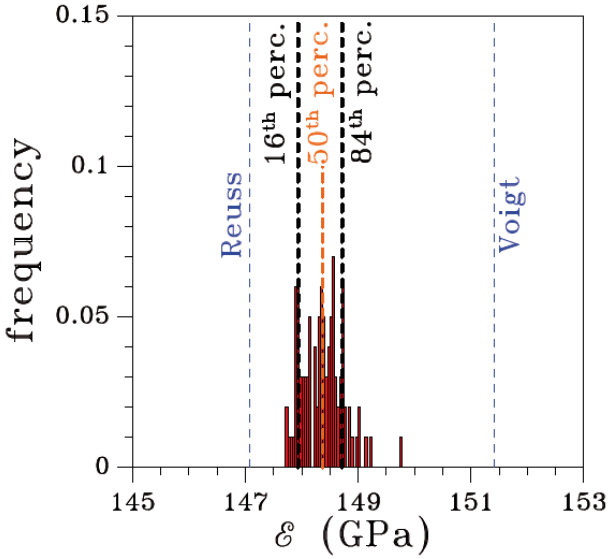

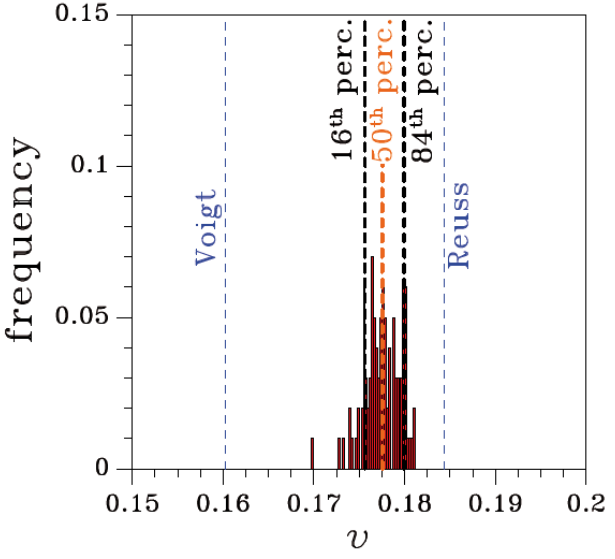

Micro-scale analysis: upscaling of elastic properties

$L = 12\ \mu\text{m},$
$\bar{s}_g = 0.6\ \mu\text{m}$

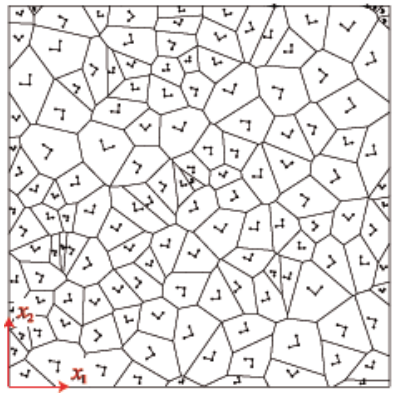

$\boldsymbol{u} = \boldsymbol{X}\boldsymbol{E}$ on ∂V

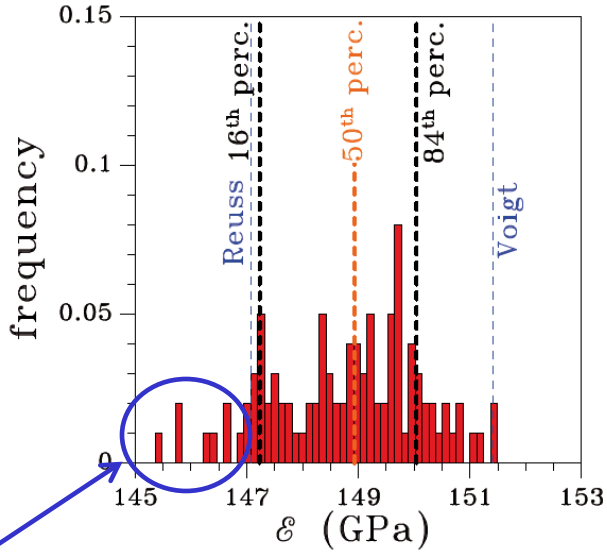

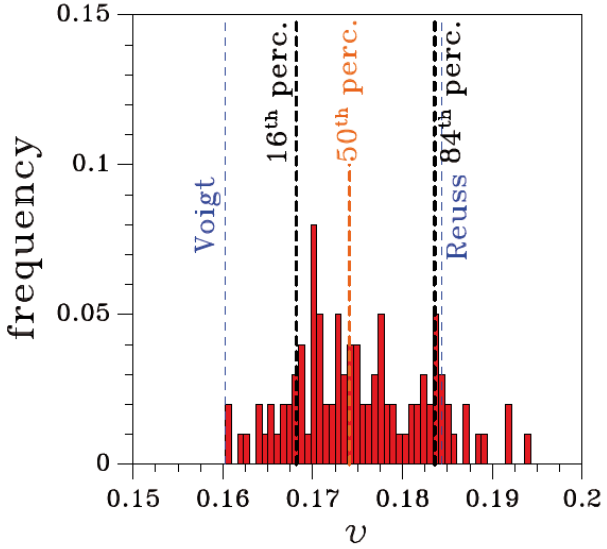

Results exceeding bounds (why?)

$$\boldsymbol{C} = \frac{1}{V}\int_V \boldsymbol{t}_\varepsilon^{\mathrm{T}}\boldsymbol{c}_l\boldsymbol{t}_\varepsilon\, dV$$

$\boldsymbol{T} = \boldsymbol{N}\boldsymbol{\Sigma}$ on ∂V

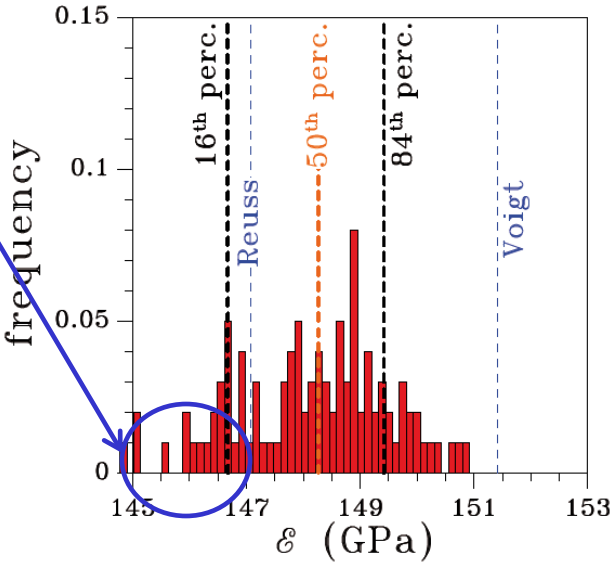

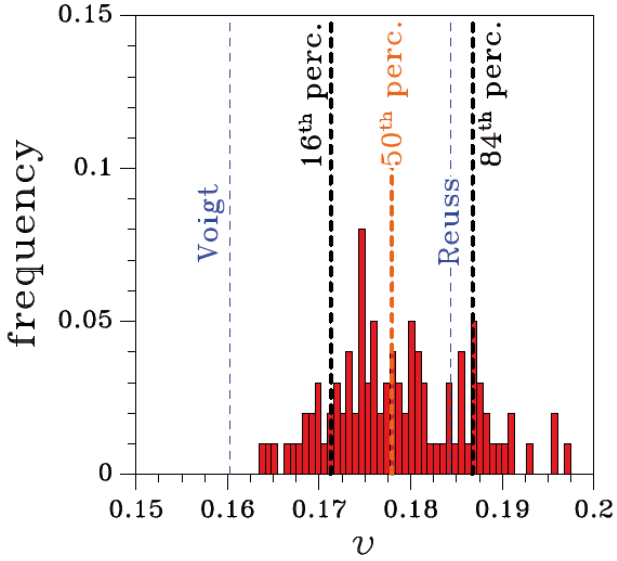

Micro-scale analysis: upscaling of elastic properties

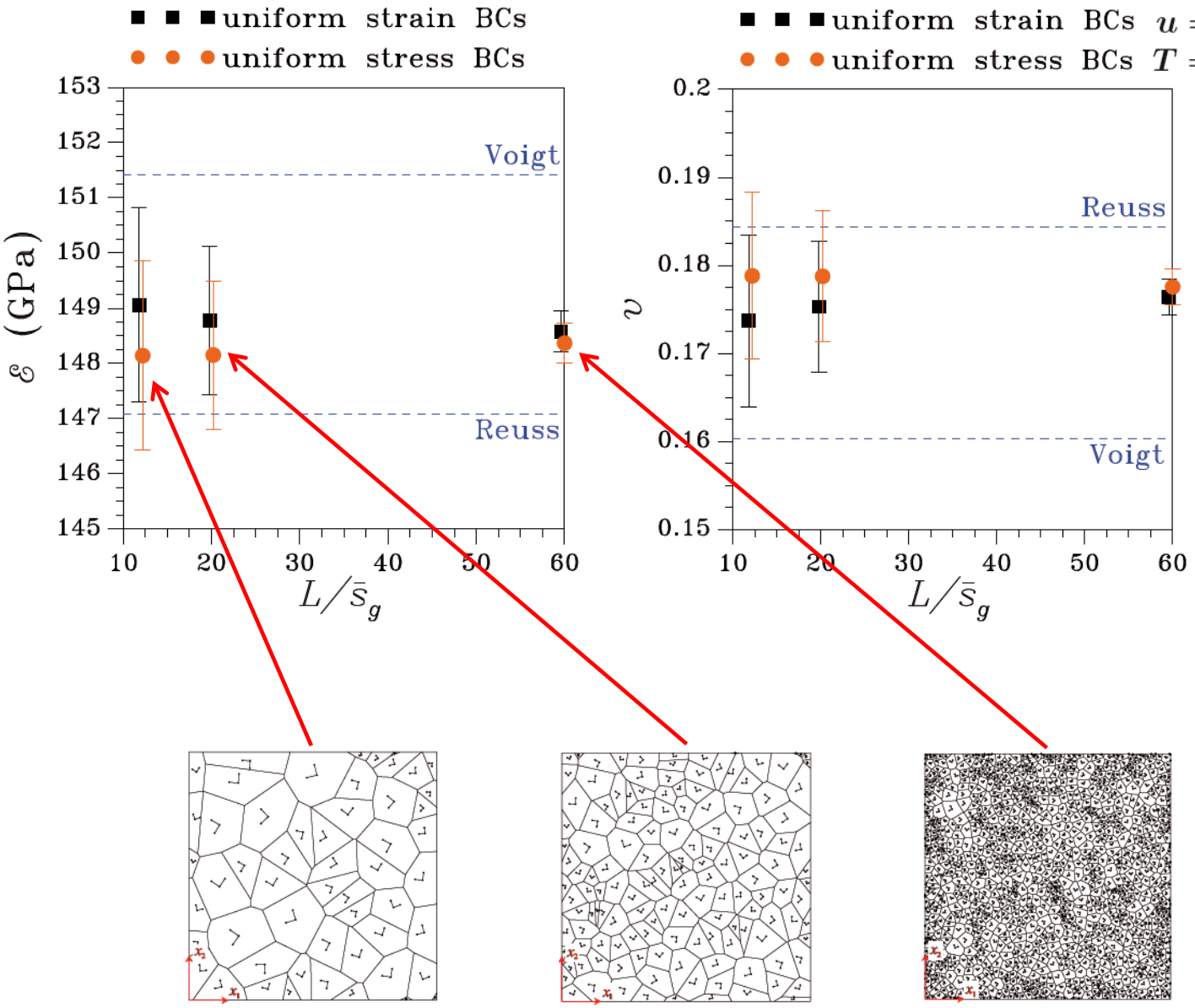

Meso-scale elastic domain (strength)

Micro-scale analysis: upscaling of elastic domain (strength)

Elastic domain of single-crystal Si (plane-stress)

3D view

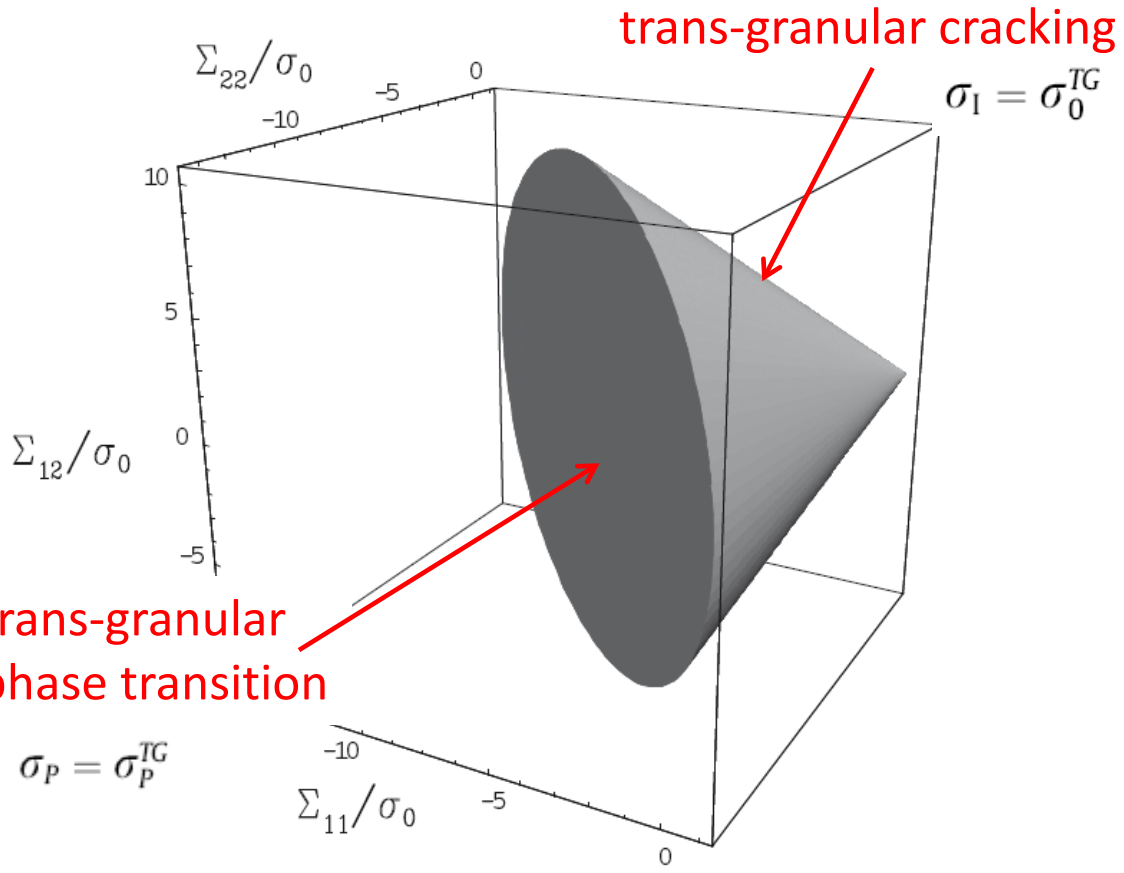

projections

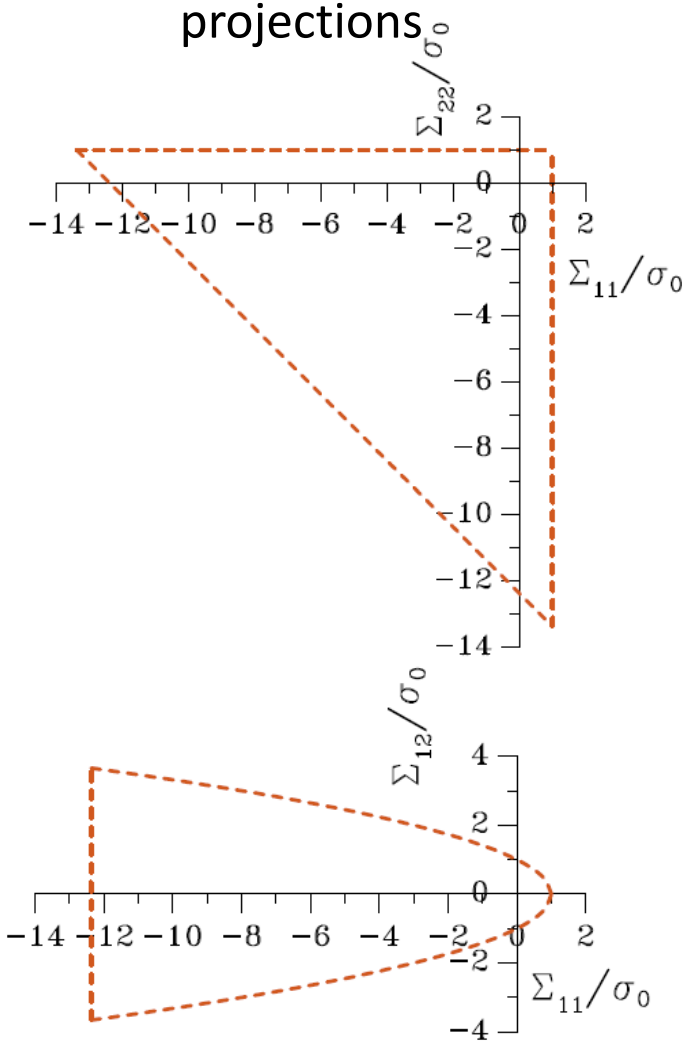

Micro-scale analysis: upscaling of elastic domain (strength)

Adding the inter-granular cracking condition $\sigma = \sqrt{\langle \sigma_n \rangle^2 + \frac{1}{\beta^2}\sigma_s^2} = \sigma_0^{IG}$ [Camacho-Ortiz], under uniform strain BCs

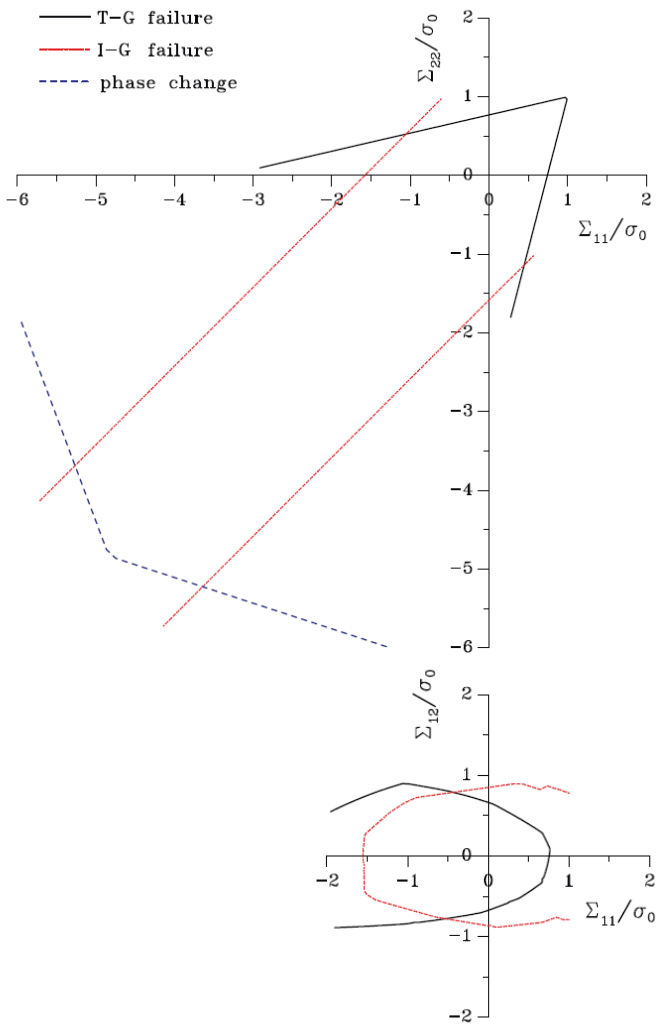

adopted space discretization to resolve stress-state along GBs

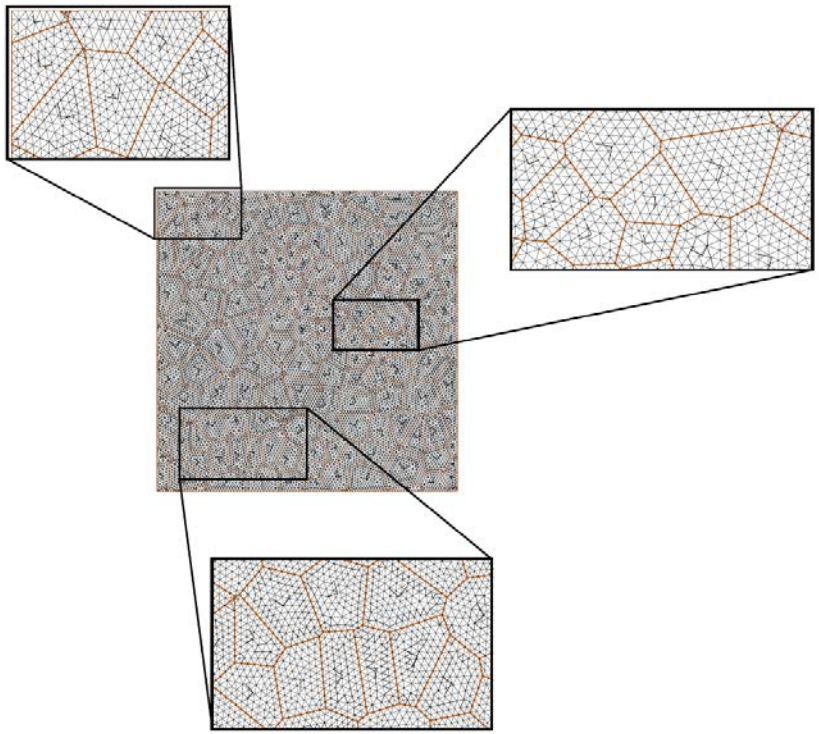

Micro-scale analysis: upscaling of elastic domain (strength)

Localization of the failing points for some stress states

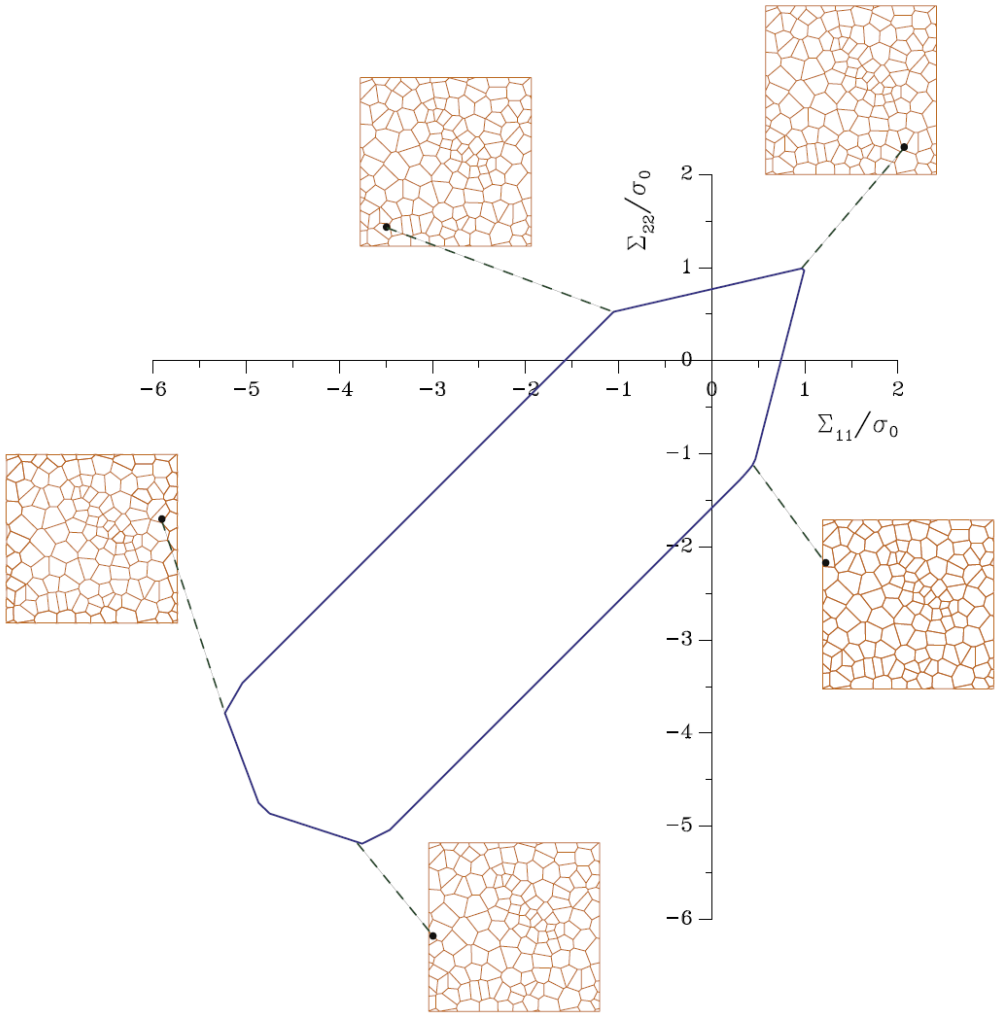

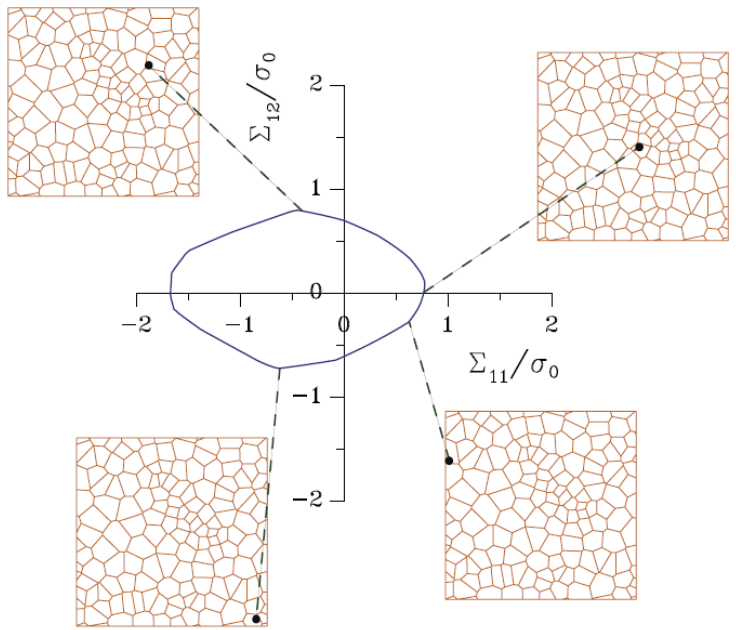

Micro-scale analysis: upscaling of elastic domain (strength)

Effect of RVE size on the shape of elastic domain ($d_e = 0.2\ \mu\text{m}$)

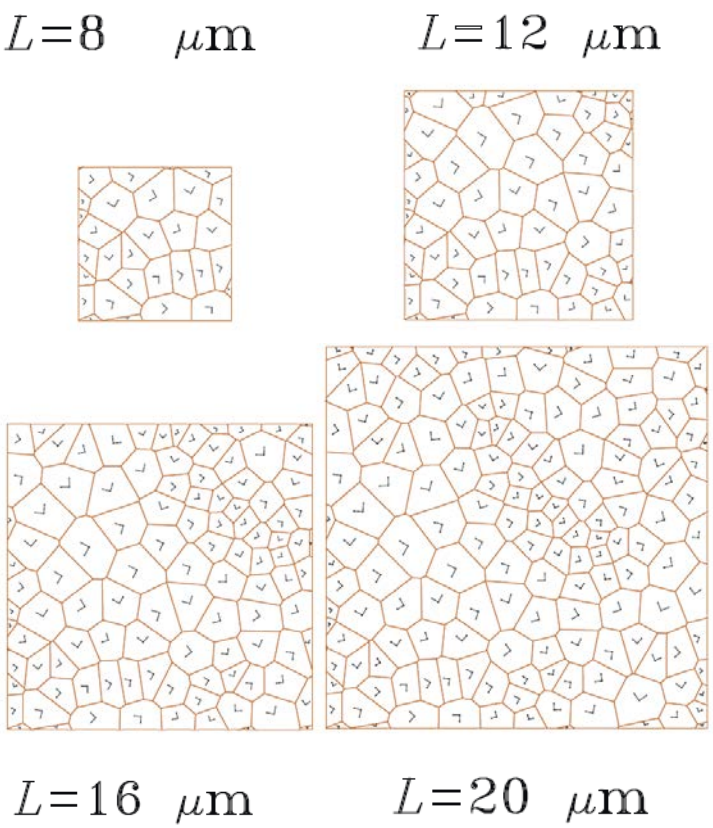

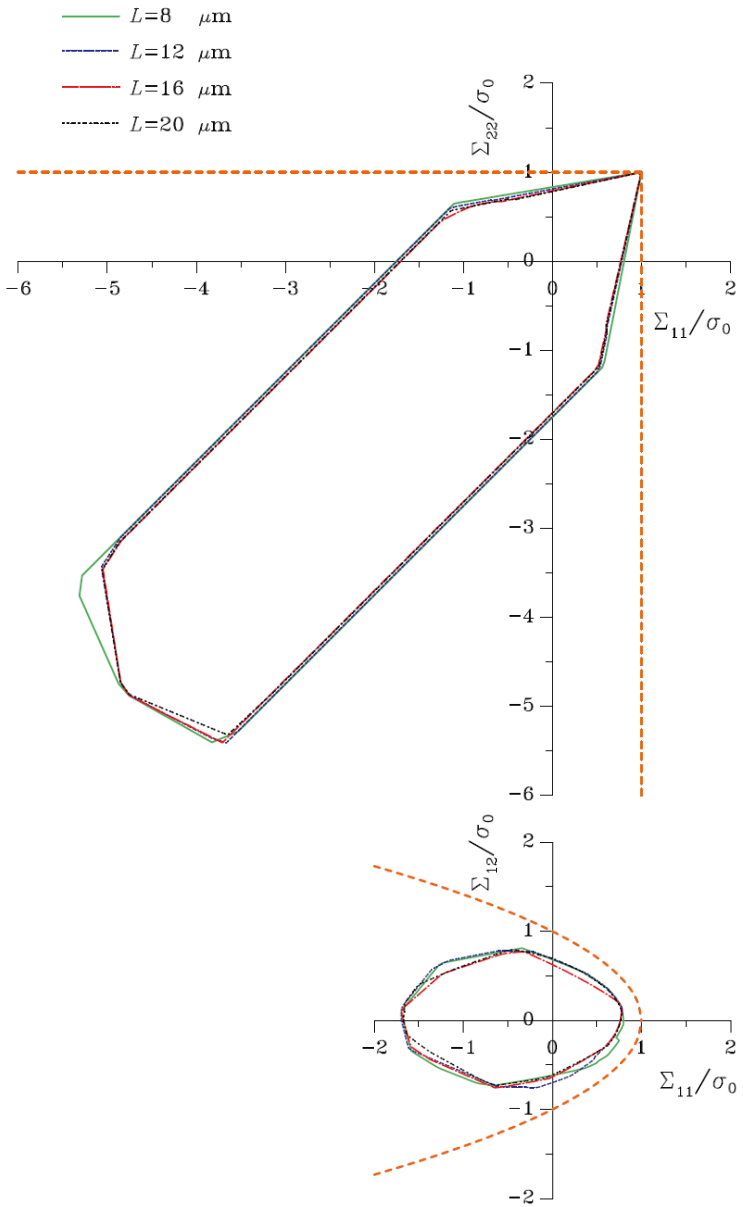

Micro-scale quasi-brittle cracking

Statics of quasi-brittle materials: principle of virtual power

Weak form of incremental equilibrium

$$\int_{\Omega\setminus\Gamma_d} \boldsymbol{\gamma}^{\mathrm{T}}\dot{\boldsymbol{\sigma}}\,\mathrm{d}\Omega = \int_{\Omega\setminus\Gamma_d} \boldsymbol{v}^{\mathrm{T}}\dot{\bar{\boldsymbol{b}}}\,\mathrm{d}\Omega + \int_{\Gamma_t} \boldsymbol{v}^{\mathrm{T}}\dot{\bar{\boldsymbol{t}}}\,\mathrm{d}\Gamma_t - \int_{\Gamma_d} [\boldsymbol{v}]^{\mathrm{T}}\dot{\boldsymbol{t}}\,\mathrm{d}\Gamma_d \qquad \forall \boldsymbol{v} \in \mathcal{U}_0$$

$\boldsymbol{v}$ is the test function

$\boldsymbol{\gamma} = \boldsymbol{C}\boldsymbol{v}$

$\mathcal{U}$ is the trial solution space
($\boldsymbol{u}$ continuous in $\Omega\setminus\Gamma_d$, possibly discontinuous along Γ_d)

$\mathcal{U}_0$ is the variation space
($\boldsymbol{v}$ continuous in $\Omega\setminus\Gamma_d$, possibly discontinuous along Γ_d, $\boldsymbol{v}=\boldsymbol{0}$ on Γ_u)

Allowing for bulk and interface constitutive models

$$\text{find } \boldsymbol{u} \in \mathcal{U}: \quad \int_{\Omega\setminus\Gamma_d} \boldsymbol{\gamma}^{\mathrm{T}}\boldsymbol{E}_{\Omega}(\boldsymbol{x})\,\boldsymbol{\varepsilon}\,\mathrm{d}\Omega + \int_{\Gamma_d} [\boldsymbol{v}]^{\mathrm{T}}\boldsymbol{E}_{\Gamma}(\boldsymbol{x})\,[\dot{\boldsymbol{u}}]\,\mathrm{d}\Gamma_d$$

$$= \int_{\Omega\setminus\Gamma_d} \boldsymbol{v}^{\mathrm{T}}\dot{\bar{\boldsymbol{b}}}\,\mathrm{d}\Omega + \int_{\Gamma_t} \boldsymbol{v}^{\mathrm{T}}\dot{\bar{\boldsymbol{t}}}\,\mathrm{d}\Gamma_t \quad \forall \boldsymbol{v} \in \mathcal{U}_0$$

Cohesive model (TG and IG cracking)

Effective displacement discontinuity [Camacho&Ortiz]:

$$[u] = \sqrt{[u]_n^2 + \beta^2 [u]_s^2}$$

opening (mode I) component

sliding (mode II) component

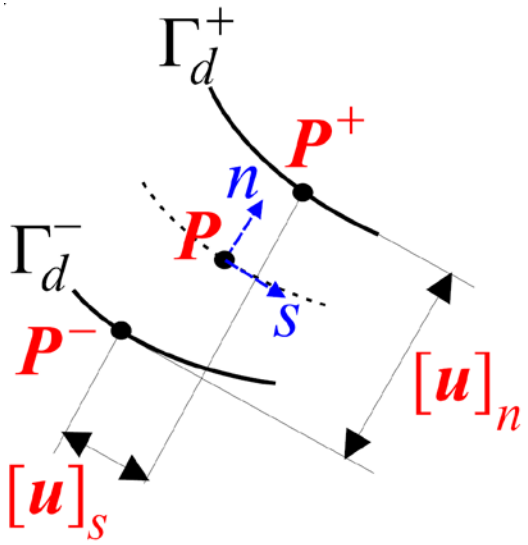

work conjugate effective traction:

$$t = \sqrt{t_n^2 + \frac{1}{\beta^2} t_s^2}$$

Irreversible effective cohesive law

- linear envelope: $t = t^{\max}\left(1 - \frac{[u]}{[u]^{\max}}\right)$
- unloading to the origin of the t-$[u]$ plane;
- fracture energy: $G = t^{\max}[u]^{\max}/2$

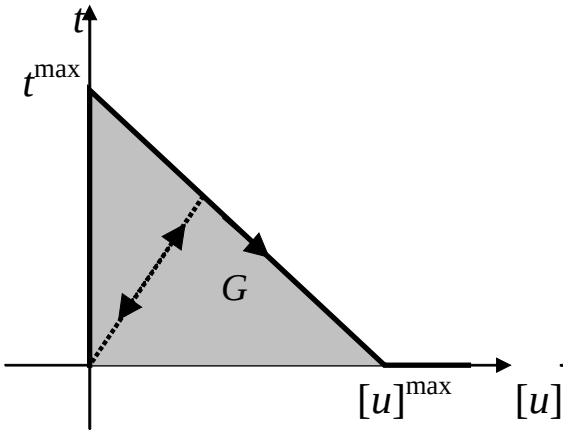

Crack description through partition of unity (X-FEM)

Enhanced FE discretized model, discontinuous along Γ_d:

nodal shape functions

$$\boldsymbol{u}^h(\boldsymbol{x}) = \sum_{i \in I} \phi_i(\boldsymbol{x})\, \boldsymbol{u}_i^0 + \sum_{j \in J} H(\boldsymbol{x})\, \phi_j(\boldsymbol{x})\, \boldsymbol{u}_j^E$$

generalized Heaviside step-function

$$\mathcal{H}(\boldsymbol{x}) = \begin{cases} +1 \text{ if } (\boldsymbol{x} - \boldsymbol{x}^*)^{\mathrm{T}} \boldsymbol{n} > 0 \\ -1 \text{ if } (\boldsymbol{x} - \boldsymbol{x}^*)^{\mathrm{T}} \boldsymbol{n} < 0 \end{cases}$$

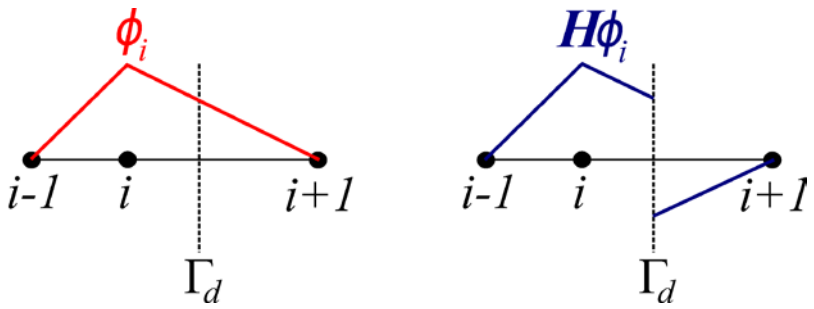

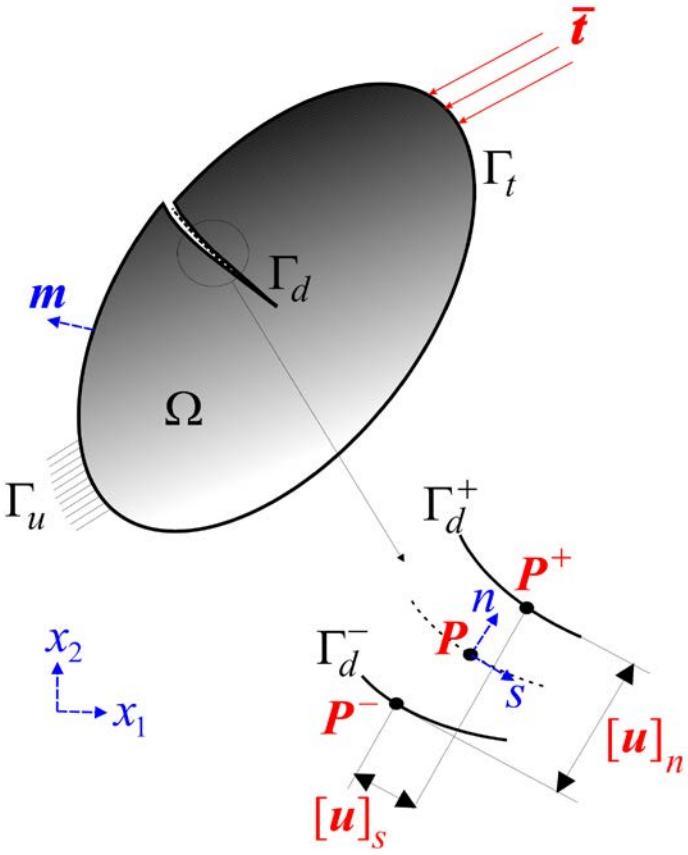

- enhancement restricted to the *j* nodes whose supports are crossed by the crack
- local refinement with limited increase of DOFs

Micro-scale analysis: anisotropic TG fracture energy

[Tanaka *et alii*, IJF]

- Transgranular fracture energy *assumed* to smoothly vary, depending on the relative orientation of crack plane and grain crystal lattice
- Transgranular strength independent of the orientation

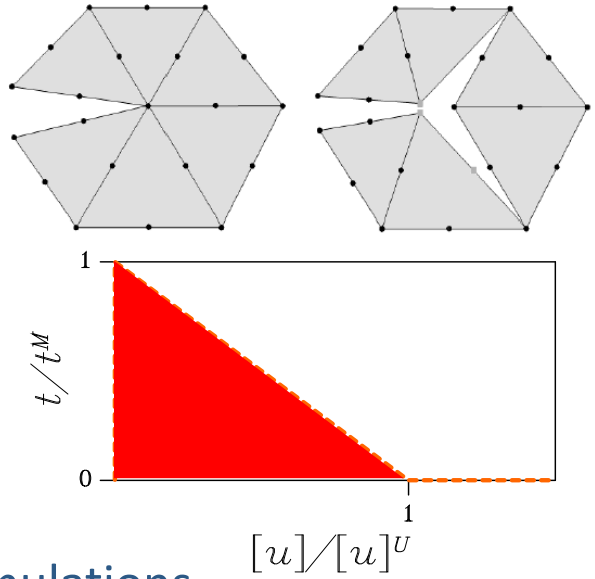

2D simulations

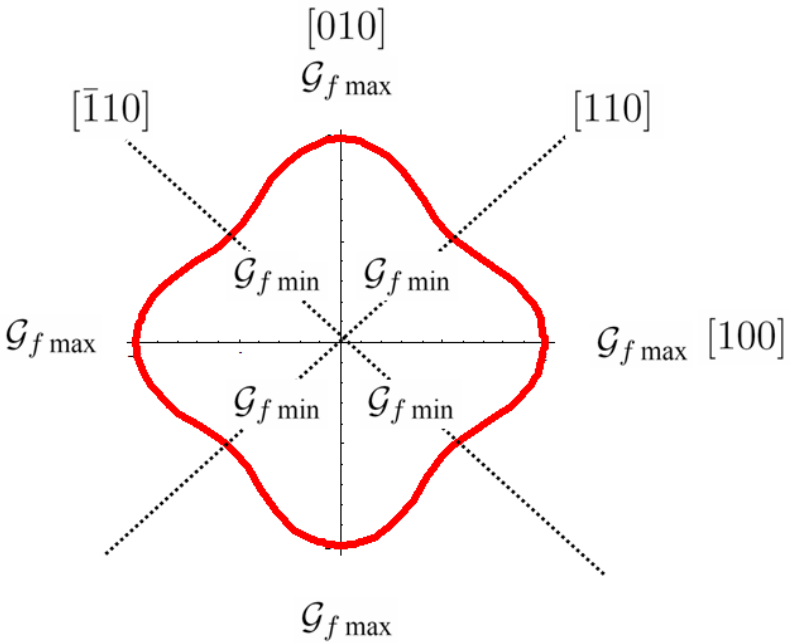

3D simulations

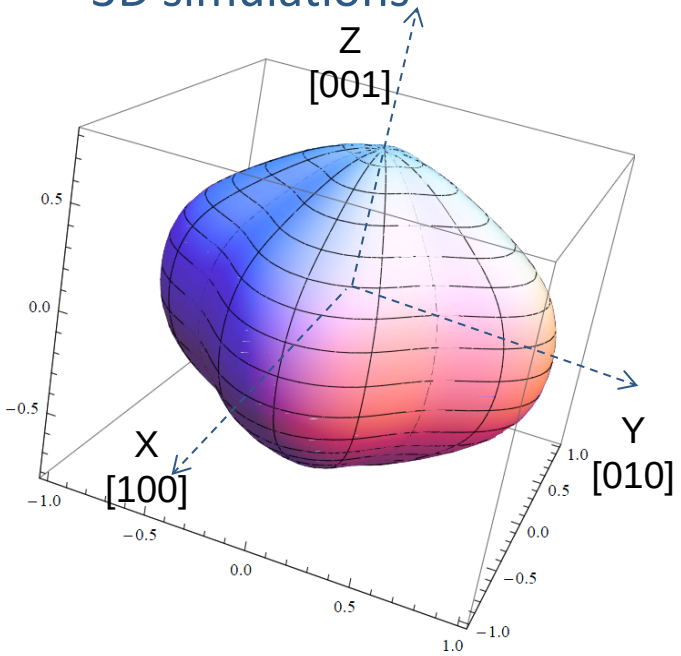

2D micro-scale analysis: typical crack evolution

Depending on the falling orientation,
crack may start from one of the two reentrant corners
at the end of each suspension spring

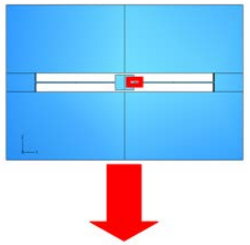

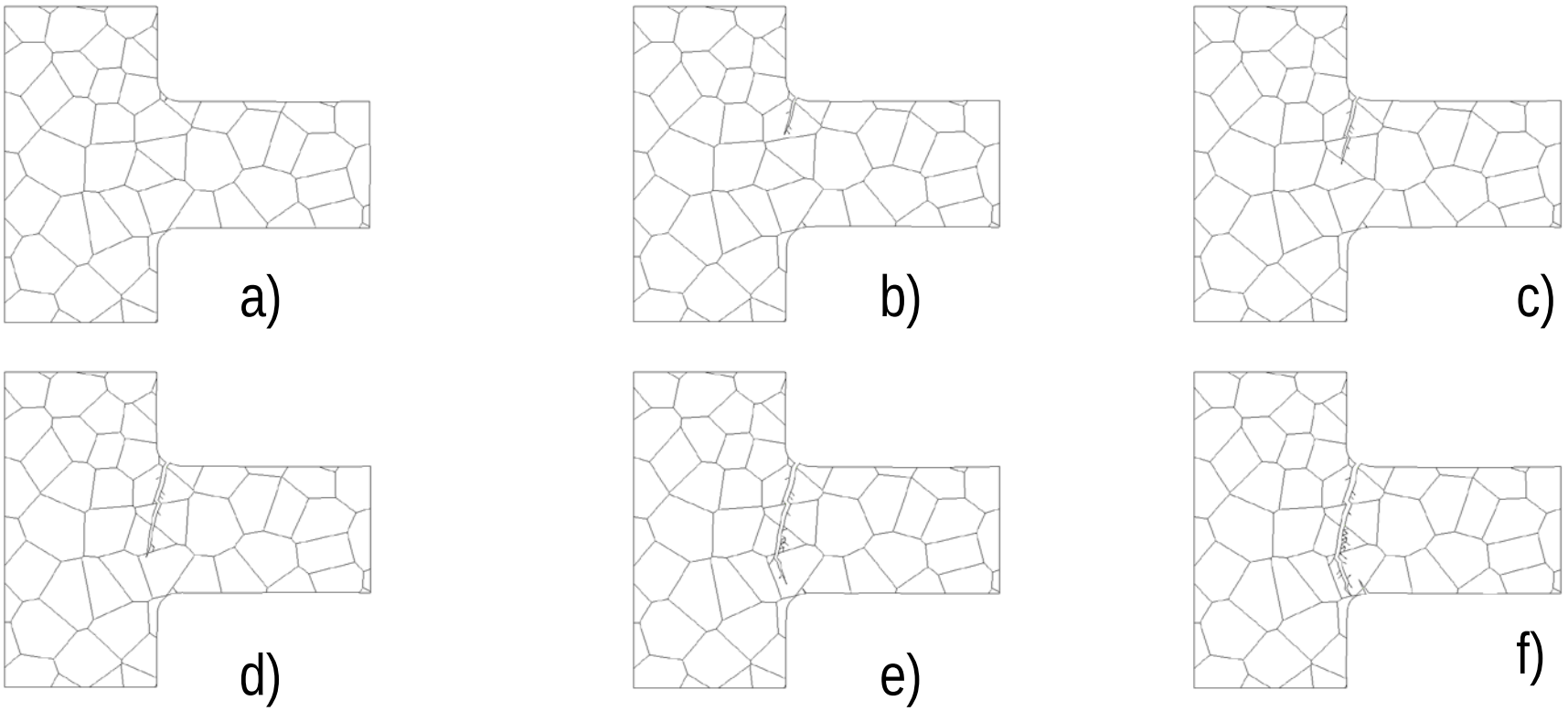

Micro-scale analysis: Monte Carlo simulations

Monte Carlo simulations are carried out with different grain morphologies and crystal orientations

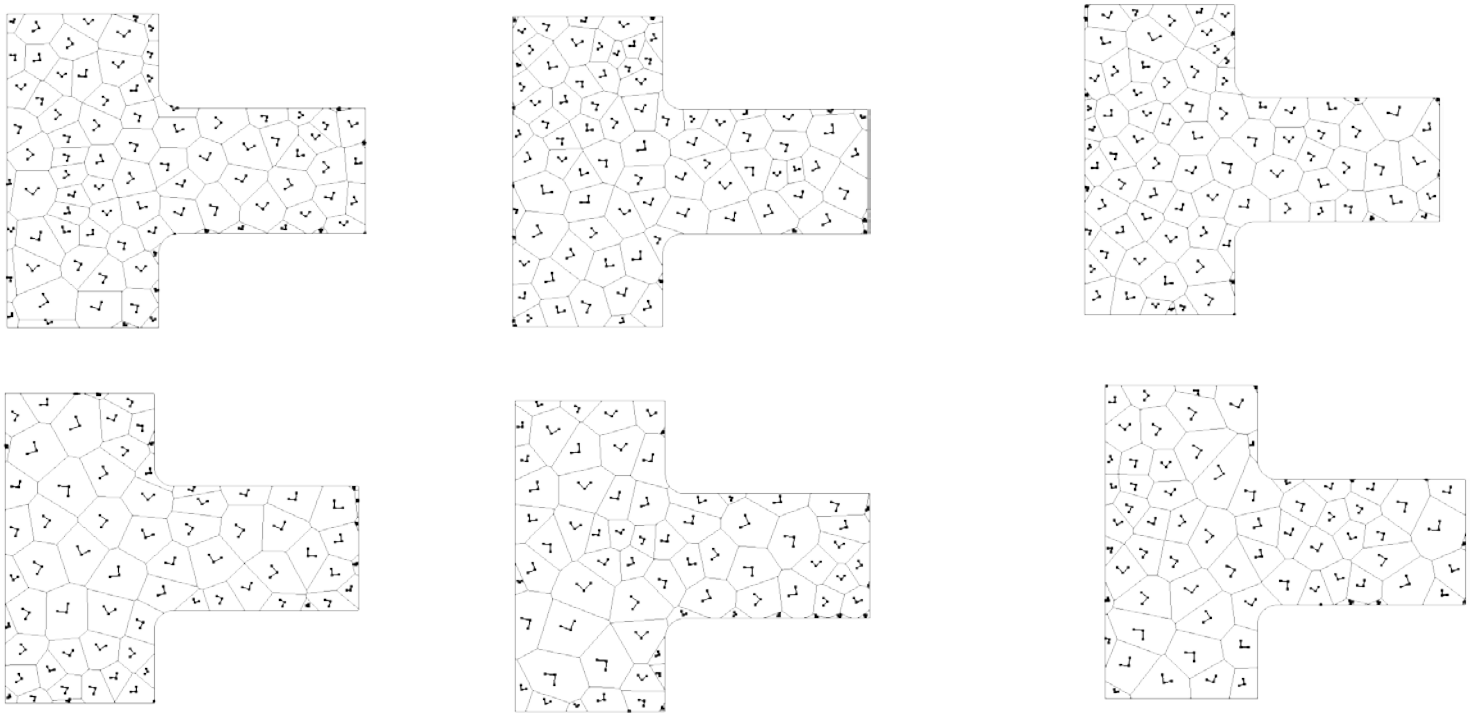

tessellation

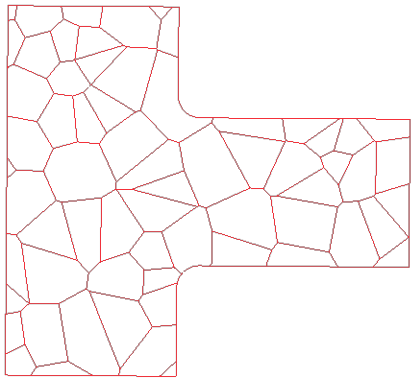

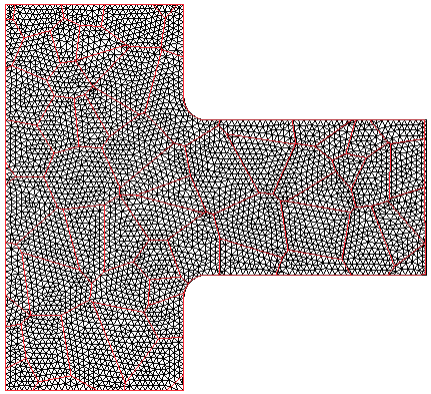

FE mesh

Micro-scale analysis: forecast of crack path at failure

Failure probability map:
at convergence of the statistics of the Monte Carlo simulation, map of probability for a crack to pass by that point

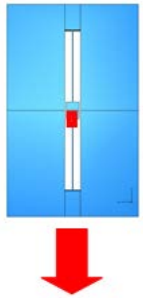

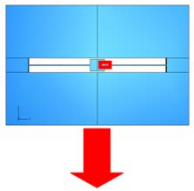

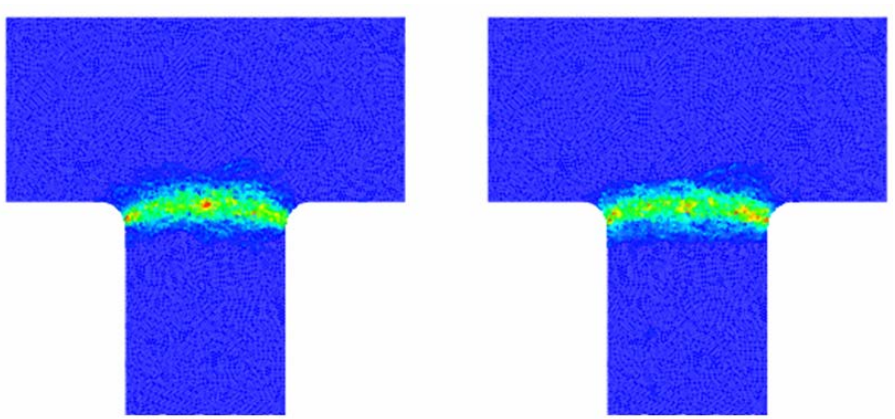

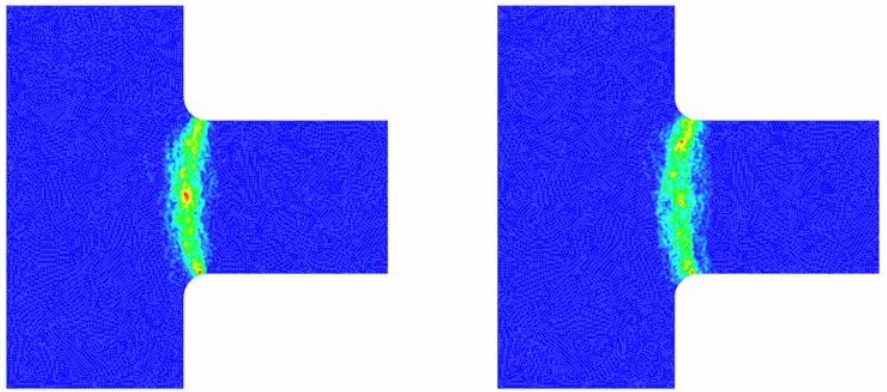

Reduced (-20%) tensile strength at grain boundaries

Reduced (-20%) tensile strength at grain boundaries

Micro-scale analysis:
3D forecast of crack pattern at failure

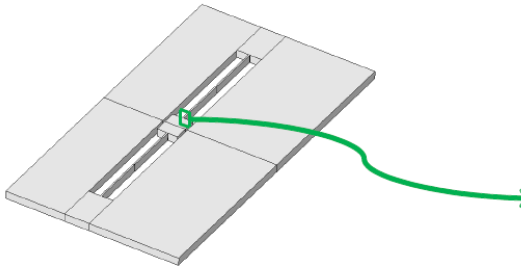

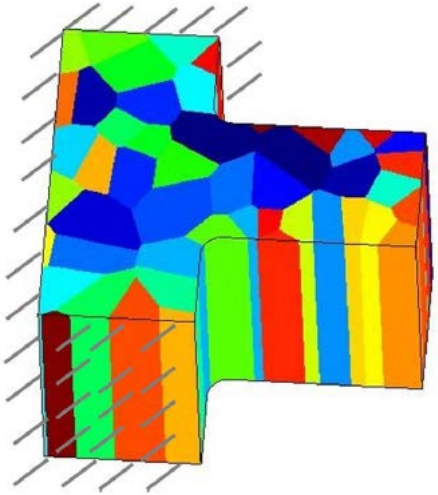

FE mesh	
Number of elements	142,648 quad tetra
Number of nodes	202,286
DOFs	**606,858**

Mesh partition into subdomains

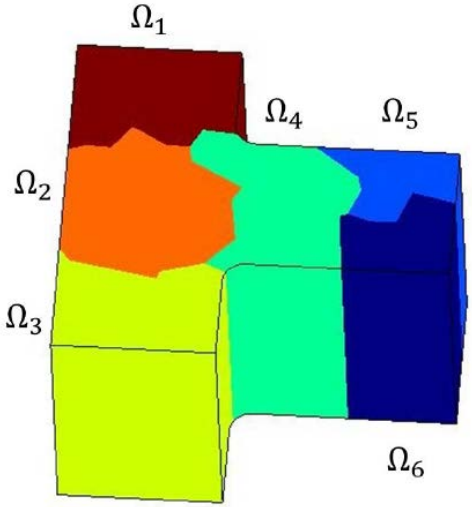

FE mesh

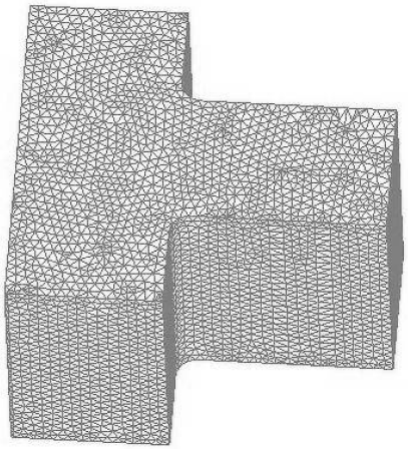

crack pattern at failure

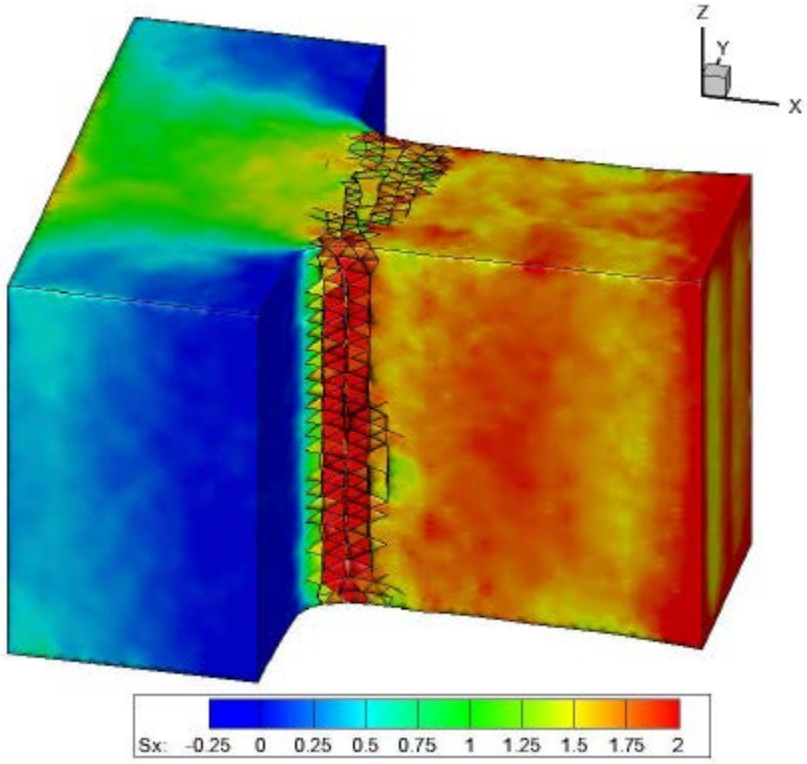

Micro-scale analysis: on-chip testing (crack and fatigue)

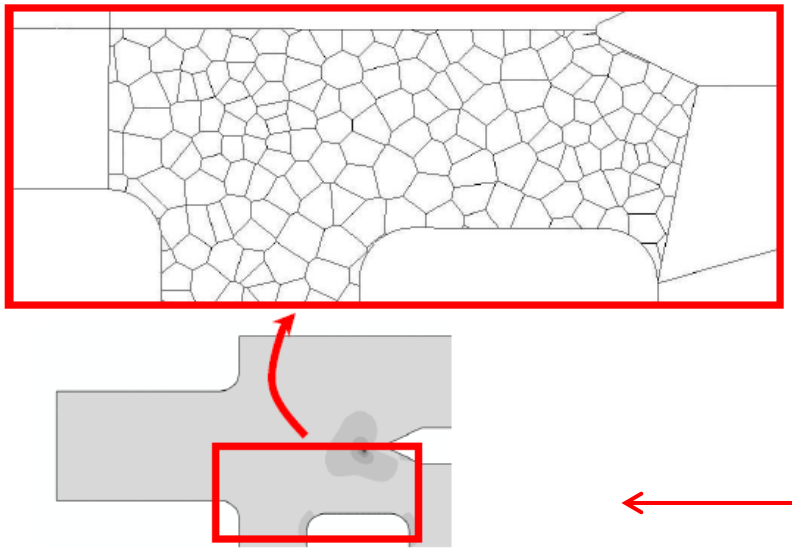

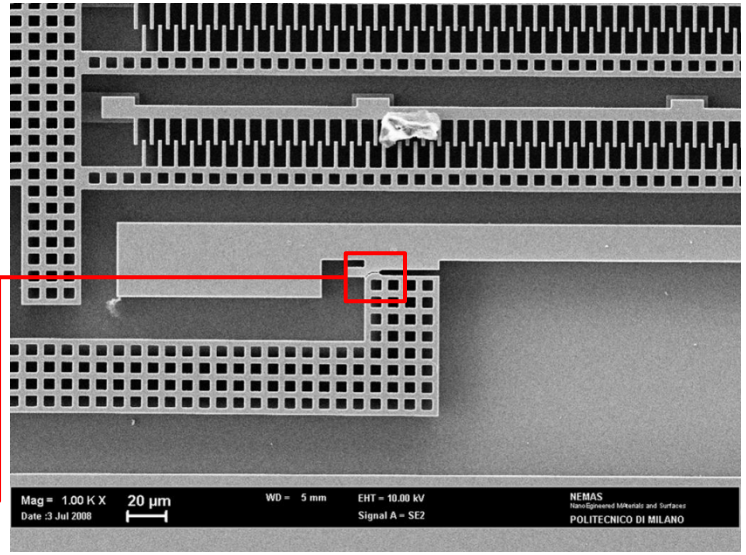

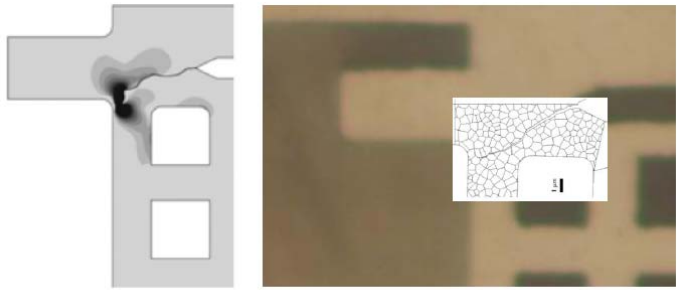

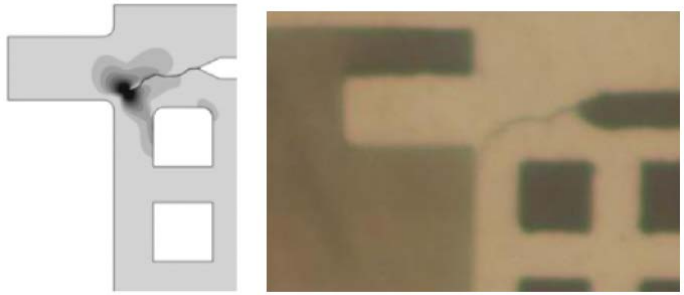

Full coupling of meso- and micro-scale analyses: a proposal based on Partition of Unity (X-FEM)

Proposal of a test-structure to measure polysilicon toughness (on-chip test)

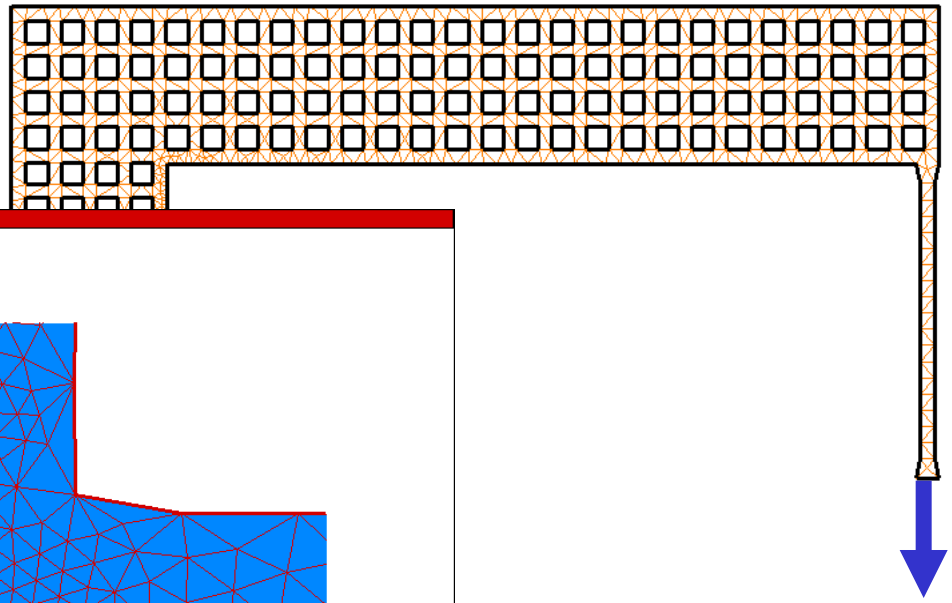

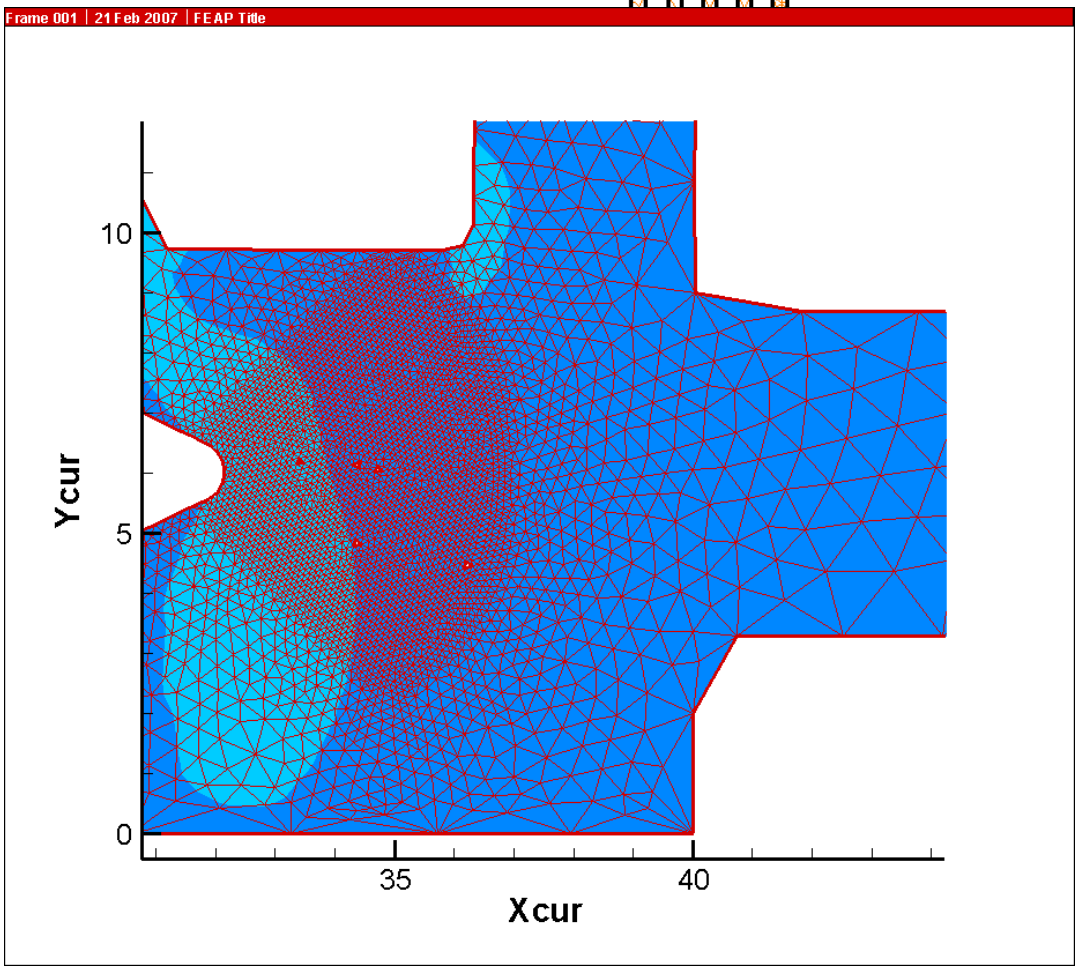

Mesh layout does not depend on crystal topology

Monte-Carlo simulations by changing the crystal morphology without modifying FE mesh

Ongoing activities

3D modeling of crack initiation and propagation:

- choice of the optimal partitioning approach (regular, automatic decomposer, grain-based, element size-based) for domain decomposition, and adaptive partitioning during crack growth
- simultaneous handling of implicit/explicit time integration techniques
- parallel implementation in an MPI environment

Multi-physics (thermo-electro-magneto-mechanical) simulations

- reduced order modeling through POD (proper orthogonal decomposition)

Acknowledgments

- Italian MIUR-PRIN projects "*Mechanics of microstructured materials: multi-scale identification, optimization and active control*" and *"Multi-scale, multi-physics and domain decomposition methods in the mechanics of microsystems and nano and micro-structured materials"*
- Regione Lombardia and CILEA-CINECA Consortium, grants: *M^2-MEMS, POLYFRAC*

Thank you for your attention!